

EFFECT OF PONGOL METHYL ETHER ON CANCER STEM CELL PHENOTYPES IN HUMAN
NON-SMALL CELL LUNG CANCER CELLS



A Thesis Submitted in Partial Fulfillment of the Requirements
for the Degree of Master of Science in Physiology
Inter-Department of Physiology
GRADUATE SCHOOL
Chulalongkorn University
Academic Year 2021
Copyright of Chulalongkorn University

ผลของพอนกอลเมทิลอีเทอร์ต่อพีโนไทป์เซลล์ต้นกำเนิดมะเร็งในเซลล์มะเร็งปอดชนิดไม่ใช่เซลล์เล็ก
ของมนุษย์



วิทยานิพนธ์นี้เป็นส่วนหนึ่งของการศึกษาตามหลักสูตรปริญญาวิทยาศาสตรมหาบัณฑิต
สาขาวิชาสารีรวิทยา (สหสาขาวิชา) สหสาขาวิชาสารีรวิทยา
บัณฑิตวิทยาลัย จุฬาลงกรณ์มหาวิทยาลัย
ปีการศึกษา 2564
ลิขสิทธิ์ของจุฬาลงกรณ์มหาวิทยาลัย

Thesis Title EFFECT OF PONGOL METHYL ETHER ON CANCER STEM
CELL PHENOTYPES IN HUMAN NON-SMALL CELL LUNG
CANCER CELLS
By Cpo.1 Arnon Silapech
Field of Study Physiology
Thesis Advisor Professor PITHI CHANVORACHOTE, Ph.D.

Accepted by the GRADUATE SCHOOL, Chulalongkorn University in Partial
Fulfillment of the Requirement for the Master of Science



..... Dean of the GRADUATE SCHOOL
(Associate Professor YOOTTHANA CHUPPUNNARAT, Ph.D.)

THESIS COMMITTEE

..... Chairman
(Associate Professor THONGCHAI SOOKSAWATE, Ph.D.)

..... Thesis Advisor
(Professor PITHI CHANVORACHOTE, Ph.D.)

..... Examiner
(Associate Professor VARISA PONGRAKHANANON, Ph.D.)

..... External Examiner
(Associate Professor Uraivan Panich, Ph.D.)

อานนท์ ศิลาเพชร : ผลของพอนกอลเมทิลอีเทอร์ต่อพีโนไทป์เซลล์ต้นกำเนิดมะเร็งในเซลล์มะเร็งปอดชนิด
 ไม่ใช่เซลล์เล็กของมนุษย์. (EFFECT OF PONGOL METHYL ETHER ON CANCER STEM CELL
 PHENOTYPES IN HUMAN NON-SMALL CELL LUNG CANCER CELLS) อ.ที่ปรึกษาหลัก : ศ. ภก.ดร.ปิติ
 จันทรวรโชติ

เซลล์ต้นกำเนิดมะเร็งเป็นเป้าหมายสำคัญในการรักษาโรคมะเร็ง การรักษาที่มุ่งเป้าหมายต่อเซลล์ต้นกำเนิด
 มะเร็งจะนำไปสู่ผลลัพธ์ทางคลินิกที่ดีขึ้น การศึกษาในครั้งนี้มีวัตถุประสงค์เพื่อทำการทดสอบความสามารถในการยับยั้ง
 เซลล์ต้นกำเนิดมะเร็งของพอนกอลเมทิลอีเทอร์สารประกอบบริสุทธิ์จากเปลือกของต้นจัน ซึ่งจะศึกษาผลในการยับยั้ง
 เซลล์ต้นกำเนิดมะเร็งโดยทำการทดสอบความสามารถในการสร้างโคโลนี, การอยู่รอดและการเจริญเติบโตในสภาวะไร้การ
 ยึดเกาะ, ความสามารถในการก่อรูปทรงกลม และการตรวจหาโปรตีนบ่งชี้ของเซลล์ต้นกำเนิดมะเร็ง โดยวิธีสัญญาณของ
 เซลล์ต้นกำเนิดมะเร็งที่เกี่ยวข้องจะถูกทดสอบด้วยวิธี Western blot, การวิเคราะห์อิมมูโนฟลูออเรสเซนส์ และ
 molecular docking โปรตีนที่มีผลต่อการทดสอบด้วยพอนกอลเมทิลอีเทอร์จะถูกนำไปวิเคราะห์ต่อด้วยวิธี
 bioinformatic ซึ่งได้แก่การวิเคราะห์เครือข่าย protein-protein interaction (PPI) ด้วย Search Tool for
 Interactions of Chemicals (STITCH) และยืนยันวิธีสัญญาณพื้นฐานด้วย Kyoto Encyclopedia of Genes and
 Genomes (KEGG) mapper ผลการศึกษาพบว่าความเข้มข้นที่ไม่เป็นพิษของพอนกอลเมทิลอีเทอร์ (5–25 ไมโครโมลาร์)
 ยับยั้งความสามารถของเซลล์มะเร็งปอดในการสร้างโคโลนี, การเจริญเติบโตในสภาวะไร้การยึดเกาะ และการก่อรูปทรง
 กลมได้อย่างมีนัยสำคัญ พอนกอลเมทิลอีเทอร์ที่ความเข้มข้น 25 ไมโครโมลาร์ สามารถลดปริมาณโปรตีนบ่งชี้ของเซลล์ต้น
 กำเนิดมะเร็ง ได้แก่ CD133 และ ALDH1A1 รวมถึง ทรานสคริปชันแฟกเตอร์ Nanog และ Oct4 ได้อย่างมีนัยสำคัญ
 และพบว่า เอเคที ซึ่งเป็นวิธีสัญญาณต้นทางที่สำคัญในการควบคุมเซลล์ต้นกำเนิดมะเร็งมีการลดลงอย่างมีนัยสำคัญ
 เช่นกัน ผล molecular docking แสดงให้เห็นว่าพอนกอลเมทิลอีเทอร์มีความสามารถในการจับกับ Akt-1 ได้สูงกว่า Akt-
 1 inhibitor (reference compound; CQW) โดยมี binding affinity อยู่ที่ -9.2 กิโลแคลอรี/โมล ผลการวิเคราะห์
 เครือข่าย STITCH พบว่ามีโปรตีนทั้งหมด 15 ชนิดที่มีปฏิสัมพันธ์ในเครือข่าย PPI โดยมี Akt-1 เป็นโปรตีนตัวกลาง และ
 ผลการวิเคราะห์ KEGG mapper พบว่าโปรตีนบ่งชี้ของเซลล์ต้นกำเนิดมะเร็งในการศึกษานี้มีความเกี่ยวข้องอย่างมากใน
 ‘signalling pathways regulating pluripotency of stem cells’ โดยมี Akt, Oct4 และ Nanog เป็นโปรตีนควบคุมที่
 สำคัญในวิธีสัญญาณนี้ นอกจากนั้นพอนกอลเมทิลอีเทอร์ (10–25 ไมโครโมลาร์) ยังสามารถยับยั้งการก่อรูปทรงกลม และ
 ลดการแสดงออกของโปรตีนบ่งชี้ที่จำเพาะของเซลล์ต้นกำเนิดมะเร็งในเซลล์มะเร็งปอดปฐมภูมิที่ได้รับมาจากผู้ป่วยได้
 อย่างมีนัยสำคัญ จากการศึกษาที่แสดงให้เห็นถึงผลทางเภสัชวิทยาใหม่และกลไกพื้นฐานทางสรีรวิทยาของพอนกอลเมทิล
 อีเทอร์ที่สามารถยับยั้งพีโนไทป์ของเซลล์ต้นกำเนิดมะเร็งในเซลล์มะเร็งปอดของมนุษย์ และอาจนำไปพัฒนาเพื่อใช้ในการ
 รักษาโรคมะเร็งปอดได้ต่อไป

สาขาวิชา สรีรวิทยา (สหสาขาวิชา)

ลายมือชื่อนิสิต

ปีการศึกษา 2564

ลายมือชื่อ อ.ที่ปรึกษาหลัก

6280075320 : MAJOR PHYSIOLOGY

KEYWORD: pongol methyl ether / cancer stem cell / lung cancer / Akt / CSC-targeting

Arnon Silapech : EFFECT OF PONGOL METHYL ETHER ON CANCER STEM CELL PHENOTYPES IN HUMAN NON-SMALL CELL LUNG CANCER CELLS. Advisor: Prof. PITHI CHANVORACHOTE, Ph.D.

Cancer stem cells (CSCs) are an important therapeutic target. The therapeutic agents targeting CSCs should lead to improved clinical outcomes. This study demonstrated the CSC suppressing activity of pongol methyl ether (PME), a pure compound from *Millettia erythrocalyx* Gagnep. CSC-suppressing effects were evaluated by colony formation assay, anchorage independent growth assay, spheroid formation assay and detection of CSC markers. The related CSC cell signals were evaluated by Western blot, immunofluorescence and molecular docking analysis. Proteins affected by PME treatment were subjected to bioinformatic analysis. Protein-protein interaction (PPI) networks were constructed by the Search Tool for Interactions of Chemicals (STITCH). The Kyoto Encyclopedia of Genes and Genomes (KEGG) mapper were used to confirm the underlying pathways. The non-toxic concentrations of PME (5–25 μ M) significantly suppressed the ability of lung cancer cells to form colonies, grow in an anchorage-independent manner and generate tumor spheroids. PME at 25 μ M significantly decreased the CSC markers (CD133 and ALDH1A1) and pluripotent transcription factors (Oct4 and Nanog). Akt, the key upstream signal of CSC control, was significantly decreased by the PME treatment. The molecular docking indicated that PME was bound to Akt-1 with a binding affinity of -9.2 kcal/mol greater than the Akt-1 inhibitor (reference compound; CQW). The STITCH network identified a total of 15 proteins interacted in PPI networks, and Akt-1 was identified as a central protein. The KEGG mapper indicated that the selected CSC markers were mostly involved in the ‘signalling pathways regulating pluripotency of stem cells’ pathway map and Akt, Oct4 and Nanog were the regulatory proteins in the dominant pathway. In addition, PME (10–25 μ M) can suppress spheroid formation and reduce CSC-specific marker expression in patient-derived primary lung cancer cells. This study revealed a novel pharmacological effect and the underlying physiological mechanism of PME that can attenuate CSC phenotypes in human lung cancer cells and may be developed for lung cancer therapy.

Field of Study: Physiology

Student's Signature

Academic Year: 2021

Advisor's Signature

ACKNOWLEDGEMENTS

Firstly, I would like to express my sincere gratitude to my advisor, Professor Pithi Chanvorachote (Ph.D.) for giving me a great understanding, expert guidance, advantage advices and kindly supports, which have given me throughout all stages of this study. Without his helpfulness and kindness this study would not be accomplished.

I would like to give a sincerely extended thanks to Associate Professor Boonchoo Sritularak of the Department of Pharmacognosy and Pharmaceutical Botany, Faculty of Pharmaceutical Sciences, Chulalongkorn University, for providing pongol methyl ether from his laboratory to be used in this study.

I would like to express my gratitude to Associate Professor Dr. Chanida Vinayanuwattikun of the Division of Medical Oncology, Department of Medicine, Faculty of Medicine, Chulalongkorn University, for providing patient-derived primary NSCLC cells from her laboratory to be used in this study.

I would like to thank to all persons of the Department of Pharmacology and Physiology, Faculty of Pharmaceutical Sciences, Chulalongkorn University to give a grateful opportunity to enroll in Master degree curriculum in inter-Department of physiology. Their helpfulness and advices are also appreciated.

Moreover, I would like to express my grateful thanks to my thesis committee, Associate Professor Thongchai Sooksawate, Ph.D., Associate Professor Varisa Pongrakhananon, Ph.D. and Associate Professor Uraivan Panich, Ph.D. for critical and important comments for enhance the coverage of thesis.

Arnon Silapech

TABLE OF CONTENTS

	Page
.....	iii
ABSTRACT (THAI).....	iii
.....	iv
ABSTRACT (ENGLISH).....	iv
ACKNOWLEDGEMENTS.....	v
TABLE OF CONTENTS.....	vi
LIST OF TABLES.....	ix
LIST OF FIGURES.....	x
CHAPTER I INTRODUCTION.....	2
CHAPTER II LITERATURE REVIEWS.....	8
1. Lung cancer.....	8
2. Cancer stem cells (CSCs).....	11
2.1 CSCs markers and proteins regulation for lung cancer.....	12
2.1.1 CD133 (Cluster of differentiation-133 or prominin-1).....	12
2.1.2 ALDH1A1 (Aldehyde dehydrogenase 1 family, member A1).....	13
2.1.3 Nanog.....	13
2.1.4 Octamer-binding transcription factor4 (Oct4).....	14
2.2 Lung CSC markers and prognosis in patients.....	14
3. Akt or protein kinase B pathway.....	17
4. Patient-derived primary lung cancer cells and their importance for CSC phenotypes test .	18
5. Pongol methyl ether.....	20

CHAPTER III MATERIALS AND METHODS	24
1. Isolation of pongol methyl ether.....	24
2. Patient-derived primary NSCLC cells preparation from malignant pleural effusion..	25
3. non-small cell lung cancer cell lines and cultures.....	26
4. Reagents and Antibodies	26
5. Cell Viability Assay	27
6. Nuclear staining assay.....	28
7. Colony Formation Assay	28
8. Anchorage independent growth assay.....	29
9. Spheroid formation assay	31
10. Western blot Analysis.....	33
11. Immunofluorescence Assay	34
12. Protein and Ligands Preparation	34
13. Molecular Docking.....	35
14. Bioinformatics Analysis; PPI Networks Integration and KEGG Pathway Maps Analyses.....	36
15. Statistical analysis.....	36
16. Ethical Consideration.....	37
CHAPTER IV RESULTS.....	42
Part 1 Investigation of CSC behaviors	42
Part 2 Effect of pongol methyl ether on CSC phenotypes	48
CHAPTER V DISCUSSION AND CONCLUSION	69
REFERENCES	78
VITA.....	92



จุฬาลงกรณ์มหาวิทยาลัย
CHULALONGKORN UNIVERSITY

LIST OF TABLES

	Page
Table 1 Lung CSC markers and prognosis in patients.....	17
Table 2 biological compounds that have an anti-cancer ability.....	22
Table 3 Administration and time schedule.....	40
Table 4 Budget.....	41
Table 5 Binding free energy of the docking simulations (kcal/mol)	63



LIST OF FIGURES

	Page
Figure 1 Pongol methyl ether, 2-(3-Methoxyphenyl)-4H-furo[2,3-h]-1-benzopyran-4-one.....	20
Figure 2 Conceptual framework of this study	38
Figure 3 Research design of this study.....	39
Figure 4 Colony Formation assay	43
Figure 5 Anchorage-independent growth.....	44
Figure 6 Primary spheroids.....	46
Figure 7 Secondary spheroids.....	47
Figure 8 Cytotoxic effect of PME.....	49
Figure 9 Apoptosis effect of PME on H460 cells.....	50
Figure 10 Effect of PME on cell proliferation by colony formation assay in H460 cells.	51
Figure 11 PME suppresses anchorage-independent growth.....	53
Figure 12 PME suppresses CSC-spheroid formation in H460 cells.....	55
Figure 13 PME suppresses CSC-spheroid formation in patient-derived NSCLC cells....	57
Figure 14 PME reduces CSC markers and transcription factors through inhibition of the ATP-dependent tyrosine kinase (Akt) signaling pathway.....	59
Figure 15 PME suppresses CSC marker (CD133) and transcription factor (Oct4) in H460 cells.....	60
Figure 16 PME suppresses CSC marker (CD133) and transcription factor (Oct4) in patient-derived NSCLC cells (MLC21-15).....	61
Figure 17 PME suppresses CSC marker (CD133) and transcription factor (Oct4) in patient-derived NSCLC cells (MLC21-16).....	62

Figure 18 Molecular Docking Simulations.....	64
Figure 19 Protein-protein interaction (PPI) networks analysis of the CSC related proteins that affected by PME treatment.	66
Figure 20 The KEGG pathway	68
Figure 21 Schematic overview of PME on lung CSC phenotypes and its related pathway.	77



LIST OF ABBREVIATIONS

%	=	percent
°C	=	degree Celsius
μM	=	micromolar
μm	=	micrometer
Akt	=	ATP-dependent tyrosine kinase
ALDH1A1	=	Aldehyde dehydrogenase 1 family, member A1
ANOVA	=	analysis of variance
CO ₂	=	carbon dioxide
CSCs	=	cancer stem cells
DMEM	=	Dulbecco's Modified Eagle's Medium
DMSO	=	dimethyl sulfoxide
FBS	=	fetal bovine serum
h	=	hour (s)
min	=	minute (s)
ml	=	milliliter (s)
mM	=	millimolar
MTT	=	3-(4,5-dimethylthiazol-2-yl)-2,5-diphenyltetrazolium bromide
NSCLC	=	non-small cell lung cancer
Oct4	=	octamer-binding transcription factor 4
P-Akt	=	phosphorylated Akt
PBS	=	phosphate-buffered saline
PI	=	propidium Iodide
PMSF	=	phenylmethyl sulfonyl fluoride
RPMI	=	Roswell Park Memorial Institute
SEM	=	standard error of the mean
TBST	=	tris-buffered saline solution with 0.1% Tween 20

CHAPTER I

INTRODUCTION

Lung cancer is a major public health problem worldwide with high incidence and mortality rate (1). The data from World Health Organization indicated that lung cancers deaths have risen from 1.2 million in 2000 to 1.8 million in 2019, and are ranked 6th among leading causes of cancer death globally (2). The major types of cancer including breast cancer, lung cancer, colorectal cancer, prostate cancer, stomach cancer, liver cancer, cervix uteri cancer esophagus cancer, thyroid cancer and bladder cancer (1). According to the Global Cancer Observatory, International Agency for Research of Cancer, lung cancer is the 1st leading cause of cancers deaths with approximately 1.7 million deaths in 2020 and more than 2 million new cases diagnosed (1). Likewise, in Thailand has a high incidence rate of lung cancer-related death, the most of which are caused by an aggressiveness of cancer (1) (3) (4). Lung cancer is a cellular genetic disorder disease in which uncontrollable cell division and that cells can metastasize to the other distant organs (5) (6). Prominent evidence shows that cancer stem cells (CSCs) in lung cancer contribute to metastasis, tumor recurrence and failure of therapy (7) (8).

CSCs or tumor-initiating cells are a minor population of cancer cells having stem cell-like abilities of self-renewal, pluripotency, and tumorigenicity (8) (9) (10). CSCs have special abilities including resisting chemotherapeutic drugs, surviving in detached conditions *via* the anoikis resistant mechanisms and initiating new tumor at secondary site (8) (11). There are several means of CSC identification including the determination of CSC related surface markers, the detection of pluripotent transcription factors and investigation of CSC-like phenotypes (12). In lung cancer, several CSC markers have been identified and widely utilized, such as CD133, aldehyde dehydrogenase1A1 (ALDH1A1), octamer-binding transcription factor 4 (Oct4) and Nanog (13) (14) (15). In terms of clinical association, the presence of these CSC markers in the tumor tissue is related to poor clinical outcomes in lung cancer patients (16) (17) (18). In addition, the expressions of Oct4, Nanog and other CSC marker proteins are correlated with high tumorigenicity and increased cancer aggressiveness (13) (19) (20). The CSCs are known to maintain their stemness through the continuous induction of pluripotency transcription factors, such as Oct4 and Nanog, and able to maintain a survival cellular signaling pathways under severe condition (21).

As CSCs become dominant targets for novel anti-cancer therapy, the upstream mechanism as well as the key determining signaling pathway that control stem cell properties have been intensively investigated. Among them, ATP-

dependent tyrosine kinase (Akt), a central signal of cell survival and proliferation, has been linked with high CSC properties in a number of cancers. The enhanced Akt signal or the constantly activated Akt frequently observed in lung cancer are associated with the evasion of cell apoptosis, chemotherapeutic resistance and increased cell dissemination (22) (23) (24) (25). Importantly, the active Akt was demonstrated to enhance CSC properties and increase tumorigenicity through the upregulation of Oct4 and Nanog (26) (27) (28) (29).

At the present, the current therapies available including surgery, radiotherapy and chemotherapy have more adverse effects and less efficient to inhibit CSCs, a major cause of cancer aggressive and recurrent (30) (31) (32) (33). Therefore, the discovery of new substances targeting CSC maintenance signals may improve the clinical outcomes in lung cancer patients and be used as an alternative therapy for disrupting CSC-driven lung cancer.

The plant-derived compound pongol methyl ether (PME) is a phenolic compound isolated from the stem bark of *Millettia erythrocalyx* Gagnep., was known as “Jan” in Thailand (34) (35). PME is a new natural product was found in 2002 (34). The stem bark of this plant is used as a traditional medicine for relieving abdominal pain (34) (35). Moreover, PME was shown to moderate antiviral activity against both of herpes simplex virus type 1 and type 2 (36). *Millettia erythrocalyx*, a member of the *Millettia* species, is the source of several biological compounds, including

millettoaloxins (A, B and C), derricidin, 5-hydroxyprunetin, pongaglabrone, ponganone I, milletenone and ovalifolin (34). It was demonstrated in previous studies that the *Millettia erythrocalyx* Gagnep has several biologically active compounds, in particular, compounds possessing anti-cancer capability against several cancer types (37) (38) (39) (40). Some of such compounds exhibit the CSC-targeting activity such as suppressing Wnt/ β -Catenin signaling (41). Moreover, other previous research showed that the phenolic compounds that have a similar chemical structure with PME, such as gigantol and chrysotoxine extract, have the potentiality to suppress lung CSCs via the Akt pathway (42) (43).

However, the CSC-targeting as well as Akt inhibition are largely under investigated. Given that the effect of PME on CSC and Akt targeted approaches has not been revealed, this study aimed at determining the CSC-targeting activity of PME and its potential underlying mechanism of action blocking CSC-inductive pathways.

Research Questions

1. How are patient-derived primary non-small cell lung cancer cells and standard non-small cell lung cancer cell lines express CSC behaviors?
2. Does pongol methyl ether could suppress CSC phenotypes including CSC markers and their behaviors in human non-small cell lung cancer cells?
3. Does pongol methyl ether suppress CSC phenotypes through Akt pathway and its downstream signaling related to CSCs?

Objectives

1. To investigate the CSC behaviors in patient-derived primary non-small cell lung cancer cells and standard non-small cell lung cancer cells.
2. To investigate the effect of pongol methyl ether on CSC behaviors in human non-small cell lung cancer cells.
3. To investigate the molecular mechanism of pongol methyl ether on CSCs in human non-small cell lung cancer cells.

Hypothesis

1. non-small cell lung cancer cells with high CSC behaviors exert the highest cancer aggressiveness.

2. Pongol methyl ether is able to diminish CSC phenotypes including CSC markers and their behaviors in human non-small cell lung cancer cells.

3. The molecular mechanisms of pongol methyl ether on suppression of CSC phenotypes in human non-small cell lung cancer cells are related to Akt pathway and it's downstream signaling.

Expected benefit and application

The results of this study provide the information of cell behaviors in patient-derived primary non-small cell lung cancer cells and standard non-small cell lung cancer cell lines with an ability of CSCs.

This study results may provide the scientific information of pongol methyl ether on regulation of lung CSC phenotypes and its molecular mechanisms including related transcription factors and marker proteins, which benefit to the further development of this novel anticancer substance.

CHAPTER II

LITERATURE REVIEWS

1. Lung cancer

Cancer is a cellular genetic disease caused by cells aggressively proliferate without control and that cells can invade the surrounding tissues and metastasize to the other distant organs (5) (6). The major types of cancer include breast cancer, lung cancer, colorectal cancer, prostate cancer, stomach cancer, liver cancer, cervix uteri cancer esophagus cancer, thyroid cancer and bladder cancer (1). Lung cancer has become an important public health problem worldwide with approximately 1.8 million cancer related deaths in 2019 (2). According to the Global Cancer Observatory, International Agency for Research of Cancer, lung cancer is the first leading cause death by approximately 1.7 million related deaths in 2020 and more than 2 million new cases diagnosed (1). In a similar way, Thailand has a high incidence rate and mortality rate of lung cancer in 2020 with 23,713 new cases diagnosed and 20,395 cases deaths, the most of which are caused by the aggressiveness of lung cancer (1) (3) (4).

Lung cancer or pulmonary carcinoma is the most common cancer worldwide, happened form normal epithelial cells continue genetic damage induced cell

proliferation without control and leading to abnormal cell growth in the various part of the lungs (1) (44). The causes of lung cancer have many factors were shown to be exposed to carcinogens such as certain chemicals, heavy metals and cigarette smoking is a big risk factor. Other causes are due to several factors include genetic factors, pulmonary fibrosis, asbestos exposure, radon gas and environmental air pollution (45) (46). Lung cancer can be classified into 2 major types based on histological characteristic; small cell lung cancer (SCLC) and non-small cell lung cancer (NSCLC) (44) (46).

Small cell lung cancer (SCLC) is found about 15% of all lung cancer patients. The major cause of this type is strongly associated with a history of cigarette smoking. Cells morphological characteristic is oat grain shaped called as oat cell cancer and its epithelial cells are smaller than other lung cancer cells. This type was often found in the large bronchial airways near the center part of the lungs (47). Small cell lung cancer is very aggressive, its growth rapidly and high rate of metastasis (48). Survival time of this type patients is 2-4 month after diagnosis so the patients usually gone very fast. The current treatment of this type has more responsive to radiotherapy and chemotherapy when compared with non-small cell lung cancer (48) (49).

Approximately 85% of all lung cancer patients are non-small cell lung cancer (NSCLC) (47) (49). Non-small cell lung cancer can be classified into 3 major subtypes,

including adenocarcinoma, squamous cell carcinoma and large cell carcinoma according to cellular morphological characteristic (50).

Adenocarcinoma is found about 40% of all lung cancer type. It's usually found in the outer part of the lungs and was to be a slow growing type (51). The patients with adenocarcinoma usually no or few noticeable symptoms and have a better prognosis when compared with the other types of lung cancer (51) (52).

Squamous cell carcinoma is usually found about 30% within early-stage of lung cancer. It's usually found in the middle part of the lungs and near a bronchial airway. The major cause of this type is related to cigarette smoking behavior like a small cell lung cancer (53).

Large cell carcinoma is the largest size cells of all lung cancer types with approximately 15% occurrence. Large cell carcinoma can be found in any part of the lungs. It has a proliferation and metastasis rate faster than the other types of non-small cell lung cancer resulting in the patients of this type have poor prognosis (54).

At the present, the current therapies of lung cancer are included surgery, radiotherapy and chemotherapy (30) (31). Although, new studies for treating lung cancer are being developed but the patient clinical outcomes have failed (32). The major cause be hiding the present of aggressive lung cancer are cancer stem cells (CSCs) (33). The main target of lung cancer therapy is an attenuation the CSCs, which

able to improved quality of life in the patients with lung cancer. Therefore, the discovery of new substance that is able to target on the CSCs might improve clinical outcome in lung cancer patients and used as an alternative therapy for disrupting aggressive lung cancer.

2. Cancer stem cells (CSCs)

Cancer cluster consist of a different population (9). CSCs or tumor initiating cells are a small cancer cell population within a tumor, which have stemness capabilities to self-renewal and pluripotency same the other types of normal stem cells (7) (9). CSCs facilitate tumor formation, metastasis, resisting cell death, resistance to chemotherapy and relapse of cancer (8) (10) (11). Currently, chemotherapeutic treatments successfully induce normal cancer cells to apoptosis but not in CSCs (8) (55). These chemotherapeutic resistance CSCs play a key role in cancer metastasis and generate a new tumor (14) (55). CSCs are being believed as the underlying cause of the high mortality rate in cancer (9) (10) (16). To define CSCs population, form whole tumor cells were able to use the CSCs protein markers specifically for each type of cancer.

2.1 CSCs markers and proteins regulation for lung cancer

Since CSCs have a stemness cellular signaling same to normal stem cells, lung CSCs were able to determine through the evaluation on normal stem cell protein markers including CD133 and ALDH1A1 (13) (56) (57). The expression of these CSCs makers can establish colonies in an anchorage-independent condition and formation detached tumor spheroids *in vitro* and *in vivo* both lung cancer patient specimens and cell lines (58) (59) (60) (61). Furthermore, these CSCs makers are related with poor clinical outcome and low survival rate in lung cancer patients (56) (62) (63).

The regulation of CSCs properties such as self-renewal and pluripotency is modulated by stem cell transcription factors both normal stem cell and CSCs (12) (19). Nanog and Oct4 are transcription factors that indicated to CSCs properties in many types of cancers including lung cancer (13) (19) (64) (65) (66). The expression of Nanog and Oct4 induced spheroids and colonies formation *in vitro* (13) (56). Moreover, their expression related with cancer aggressiveness and increases new tumor genesis *in vivo* (67) (68) (69) (70).

2.1.1 CD133 (Cluster of differentiation-133 or prominin-1)

CD133 is a cell surface transmembrane glycoprotein have a molecular weight of 120kDa, consists of 865 amino acids on single chain polypeptide (13). The

expression of these protein has been reported as a marker of stemness phenotypes is several cancers (13) (56). In lung cancer, CD133 is an importance stemness marker presented significantly high capabilities of tumor aggressiveness, chemoresistance, metastasis and tumorigenesis characteristics (62) (71) (72). In addition, overexpression of CD133 has been related with higher tumor stage and poor prognosis in lung cancer patients (56) (73) (74).

2.1.2 ALDH1A1 (Aldehyde dehydrogenase 1 family, member A1)

ALDH is an enzyme was responsible to detoxification the oxidation of aldehydes into carboxylic acids (75). ALDH1A1 is a member of the ALDH1 family have a molecular weight of 55kDa and 501 amino acids (13) (56). The expression of this protein found in several cancers which increase tumor aggressiveness, drug resistance and cancer recurrence, through advertised function in detoxification of chemotherapeutic drugs (56) (75) (76) (77) (78). In lung cancer cells, ALDH1A1 expression is associated with stemness properties such as self-renewal, pluripotency, clonogenicity and tumorigenicity (56) (79) (80) (81).

2.1.3 Nanog

Nanog is a transcription factor plays an important role for self-renewal and pluripotent in both normal stem cells and CSCs (82) (83). Nanog have a molecular weight of 42kDa and 350 amino acids (13) (56). Responsibility of this protein is

associated with CSCs phenotype characteristic in various cancers (13) (19) (83) (84). The overexpression of Nanog promotes lung cancer aggressiveness and related with poor clinical prognosis in patients (13) (65) (84) (85).

2.1.4 Octamer-binding transcription factor4 (Oct4)

Oct4 is a transcription factor have a molecular weight of 45kDa including 4 isoforms; Oct4A, Oct4B-190, Oct4B-265, and Oct4B-164 (13). Oct4A was encountered in oocytes and regulates stemness in embryonic stem cells, which related in self-renewal and pluripotent ability (13) (86). The other forms of Oct4B are involved in cell stress and differentiation (13). The high expression of Oct4 was related with CSCs phenotypes including spheroid formation, colony formation, tumor formation and associated with high CSCs protein marker expression (13) (87) (88). Moreover, overexpression of Oct4 was extremely correlated with higher aggressive tumors, metastasis, cancer relapse and poor prognosis in lung cancer patients (89) (90) (91) (92).

2.2 Lung CSC markers and prognosis in patients

Many previous research indicated that the expression of lung CSC-related markers were associated to a poor clinical outcome among NSCLC patients, suggesting their potential use as prognostic markers such as CD133, ALDH1A1, CD44, ATP-binding cassette superfamily G member 2 (ABCG2), Oct4, Nanog and Sox-2 (19)

(93) (94). The CSCs are known as a cause of chemo-radio resistant and cancer aggressiveness (8). These studies revealed that the expression of CSC makers and transcription factors in lung cancer suggest the aggressive of cancer cells and related to a poor clinical outcome in patients (table 1).

CSC makers	Description and Prognostic in lung cancer	References
CD133 or Prominin-1	<ul style="list-style-type: none"> - A five-membered transmembrane glycoprotein. - Cell regeneration and differentiation. - Linked to poor prognosis in patients with NSCLC. - Higher tumor stage in adenocarcinoma. 	(74) (95)
ALDH1A1	<ul style="list-style-type: none"> - A cytosolic isoenzyme, is a member of the ALDH family involving in aldehyde detoxification. - Protection of CSCs against the oxidative aldehyde. - Correlated with poor clinical outcome and advanced stage of disease in NSCLC. 	(63) (96)
Cluster of differentiation-44 (CD44)	<ul style="list-style-type: none"> - A cell surface glycoprotein involved in cell-to-cell interactions, adhesion and motility of cells. - Enhanced tumorigenicity, tumor generations and increased chemoresistance. - High rates of CD44 expression were prognostic in adenocarcinomas 	(97) (98)

CSC makers	Description and Prognostic in lung cancer	References
ATP-binding cassette superfamily G member 2 (ABCG2)	<ul style="list-style-type: none"> - The transporter works by using energy from ATP to drive the active transport of drug metabolites and other compounds across the cell membrane. - A powerful resistance mechanism that greatly contributes to chemoresistance of CSCs. - Associated with high pathological grade of tumor and poor prognosis outcome of patients. 	(99) (100)
Octamer-binding transcription factor4 (Oct-4)	<ul style="list-style-type: none"> - A POU domain-containing transcription factor. - Maintaining and regulates the stemness of embryonic stem (ES) cells capacity. - Highly aggressive tumors, poor prognosis patients, and relapse cancer. 	(87) (90)
Nanog	<ul style="list-style-type: none"> - A transcription factor responsible for maintaining the self-renewal capacity of ES cells in embryonic development. - Promotes tumorigenicity, associated with tumor progression, resistance to chemo-radio therapy and relapse. - Predicted worse prognosis for lung cancer patients. 	(65) (101)

CSC makers	Description and Prognostic in lung cancer	References
Sex determining region Y-box 2 (Sox2)	<ul style="list-style-type: none"> - A member of the Sox transcription factor that occupies self-renewal maintaining genes. - Development, growth and differentiation of cells. - Associated with chemo-resistance, cancer migration and anchorage-independent growth. - Marker for poor prognosis in lung cancer. 	(102) (103)

Table 1 Lung CSC markers and prognosis in patients

3. Akt or protein kinase B pathway

Protein kinase B or Akt is a downstream family member of Phosphatidylinositol-3-kinase (PI3K) signaling (104) (105). The Akt can be activated by several cytokines or agonists such as growth factors (105) (106). Activated Akt is able to control a crucial cellular function in many physiological and pathological conditions including cell survival, growth (increase size of cell), proliferation (increase number of cell), metabolism, cell cycle progression and self-renewal ability (25) (107) (108). The activity and expression of Akt was strongly associated to an aggressiveness in lung cancer (109) (110). Akt is a serine/threonine kinase protein, has a 60kDa molecular weight and consists of 480 amino acids (111) (112) (113). Akt is involved in many

cellular mechanisms, both normal cells, normal stem cells, cancer cells and CSCs (114) (115).

In many studies, Akt was reported to play a key role in regulating CSCs abilities (25) (114) (116) (117). Akt signaling pathway activation promoted CSC phenotypes and their behaviors, many studies showed that Akt able to regulate the CSC markers through the CSC transcription factors (25) (114). The regulation of CSC transcription factors including Nanog and Oct4 through phosphorylation was demonstrated to be a downstream regulation of Akt signaling pathway which causing of the tumorigenicity and cancer aggressiveness (25) (27) (82) (118) (119). The inhibition of Akt activity able to attenuated an activity of these transcription factors and other CSC marker proteins which resulting in the CSCs phenotype diminish (29) (114).



4. Patient-derived primary lung cancer cells and their importance for CSC phenotypes test

Many previous studies referred to the limited success on lung cancer treatment, radio-chemotherapy resistant, metastasis, tumor recurrence and cancer progression that mainly caused by CSCs (7) (8). For investigated the understanding of CSCs physiology, genetic differentiations, protein markers discovery and analyze potential of new therapeutic agents, the cancer cell lines have been to used (120).

However, has controversial issue about cancer cell lines correlation with primary cancer cells from which they were derived such as cancer phenotypic change and loss of cell heterogeneity after multiple passages subculture (121) (122). Moreover, cancer cell lines experiment *in vitro* may not represent to a clinical status in cancer patients correctly (123). Thus, for investigated the CSC phenotype and its compound effects only in *in vitro* cancer cell line experiments may not be sufficient. While in the other studies were show that cancer cell lines can maintain and reserve mostly genetic characteristics, protein expression level and epigenetic change of original tumor tissues (124) (125). In addition, primary cancer cells derived from the patient are so difficult to sustaining culture for a long time. This is an important limitation in *in vitro* CSC phenotypes testing.

Below this reason, both of patient-derived primary NSCLC cells and standard NSCLC cell lines are used in this study and aimed to understanding CSCs physiology in clinical of NSCLC patients.

5. Pongol methyl ether

PME, 2-(3-Methoxyphenyl)-4H-furo[2,3-h]-1-benzopyran-4-one, is a phenolic compound extracted from the stem bark of *Millettia erythrocalyx* Gagnep., is known as “Jan” in Thailand (34) (35). A chemical formula of PME is $C_{18}H_{12}O_4$ and its molecular weight is 292.3 g/mol, were shown in Figure 1.

PME is a new natural product was found in 2002 (34). The stem bark of this plant is used as a traditional medicine for relieving abdominal pain (34) (35). Moreover, PME was shown to moderate antiviral activity against both of herpes simplex virus type 1 and type 2 as compared with acyclovir. Expressed with 50% effective dose at a concentration of 70.5 μM in HSV-1 and 50% effective dose at a concentration of 132.8 μM in HSV-2 (36).

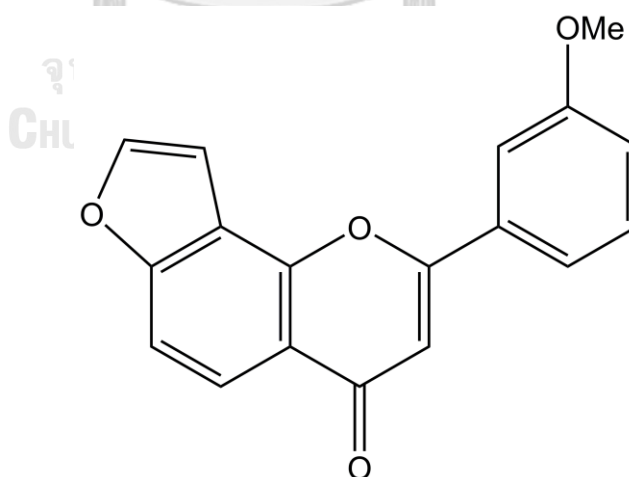
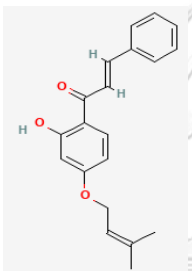
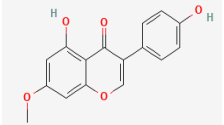


Figure 1 Pongol methyl ether, 2-(3-Methoxyphenyl)-4H-furo[2,3-h]-1-benzopyran-4-one

Millettia erythrocalyx, a member of the *Millettia* species, is the source of several biological compounds, including millettocalyxins A, B and C, and derricidin, 5-hydroxyprunetin, pongaglabrone, ponganone I, milletenone and ovalifolin (34). Previous studies indicated that the biological compounds from this plant have an anti-cancer ability in several cancer types including;

Compounds	Structure	Cell types	Anti-cancer properties	Ref.
Derricidin (C ₂₀ H ₂₀ O ₃)		CRCs cell lines (HCT116 and DLD-1)	Suppress colon cancer cell growth through inhibit Wnt/ β -Catenin signaling	(37)
Prunetin (C ₁₆ H ₁₂ O ₅)		Human Hepatoma HuH-7 Cells	Induces apoptosis and caspase-3-like activity.	(38)
		Human gastric cancer cell line AGS	Induces cell death in gastric cancer cell with potent anti-proliferative properties via receptor interacting protein kinase 3 (RIPK3)	(39)

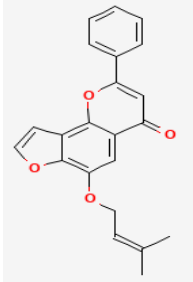
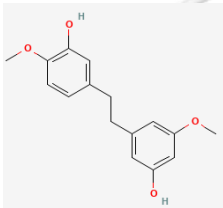
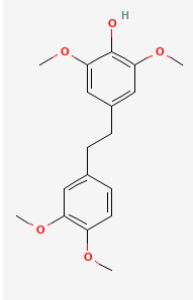
Compounds	Structure	Cell types	Anti-cancer properties	Ref.
Ovalifolin (C ₂₂ H ₁₈ O ₄)		Breast-adenocarcinoma cell lines MCF-7 (ER +ve) MDA-MB-231 (ER -ve)	Antiproliferative activity and induction of apoptosis in estrogen receptor-positive and negative human breast carcinoma cell lines	(40)
Gigantol (C ₁₆ H ₁₈ O ₄)		Human NSCLC cell lines, NCI-H460	Reduces CSC Phenotypes and markers including CD133 and ALDH1A1 in Lung Cancer Cells by suppressing the activation of protein kinase B (Akt) signal.	(42)
Chrysotoxine (C ₁₈ H ₂₂ O ₅)		Human NSCLC cell lines NCI-H460 and NCI-H23	suppresses CSCs ability and inhibits CSC markers (CD133, CD44, ABCG2, and ALDH1) and pluripotency transcription factor Sox2 via the Src/Akt signal in human lung cancer cells	(43)

Table 2 biological compounds that have an anti-cancer ability

Some of the listed compounds exhibit the CSC-targeting activity such as suppressing Wnt/ β -Catenin signaling (41). Moreover, other previous research showed that the phenolic compounds that have a similar chemical structure with PME, such as gigantol and chrysotoxine extract, have the potentiality to suppress lung CSCs *via* the Akt pathway (42) (43).

However, the effect of PME on CSC phenotypes and the underlying mechanisms were not reported. Therefore, this study aimed to examine whether PME was able to attenuate the CSC phenotypes in *in vitro* human NSCLC cells and to examine the underlying molecular mechanism pathway.

CHAPTER III

MATERIALS AND METHODS

1. Isolation of pongol methyl ether.

PME was extracted from the stem bark of *Millettia erythrocalyx* Gagnep. as previously indicated (34). The dried and coarsely powdered of this stem bark (2 kg) were extracted with ethyl acetate and MeOH to give a viscous mass (37 g) of dried extract after evaporation of the organic solvent under reduced pressure. The materials were subjected to vacuum-liquid chromatography over silica gel (ethyl acetate-hexane gradient) to give A-I fractions. Fraction F8 (570 mg) was separated by column chromatography on silica gel (gradient elution ethyl acetate-pet. ether 20:80 to 30:70) to afford 139 mg of PME as a yellowish powder (Rf 0.38, silica gel, ethyl acetate-pet. ether 2:3). The structural of PME used in this study was determined a purity through analysis of nuclear magnetic resonance (NMR) spectroscopy. PME was prepared in dimethyl sulfoxide (DMSO) (Sigma Chemical, St. Louis, MO, USA) as a stock solution, and diluted with RPMI media to achieve the desired concentrations. The final concentrations of DMSO in all experiments were less than 0.1% , that not cytotoxicity.

2. Patient-derived primary NSCLC cells preparation from malignant pleural effusion.

Thai NSCLC patients with malignant pleural effusion who had been diagnosed and receiving treatment at the King Chulalongkorn Memorial Hospital, were prospectively enrolled in the study. Informed consent was obtained from all patients and this study was approved by the Ethics Committee of the Faculty of Medicine, Chulalongkorn University, Bangkok, Thailand (IRB 365/62) (Date of Approval: 31 July 2020). The malignant pleural effusion was collected from a part of standard diagnosis practice and clinical treatment by thoracentesis.

In part 1 investigation, the samples were centrifuged at 300 g for 10 min, at 4 °C, and cell pellets were resuspended in Roswell Park Memorial Institute (RPMI) 1640 medium (Gibco, Grand Island, NY, USA) with 10% fetal bovine serum (FBS) (Merck, DA, Germany), 2 mM L-glutamine (Gibco, Grand Island, NY, USA), and 100 units/mL of each of penicillin and streptomycin (Gibco, Grand Island, NY, USA). The cell viability was determined by Trypan Blue exclusion dye. All cells were cultured in Roswell Park Memorial Institute (RPMI) 1640 medium (Gibco, Grand Island, NY, USA) at 37 °C with 5% CO₂.

In part 2 investigation, the samples were culture onto a 24-well ultra-low attachment plate in serum-free RPMI media and incubated at 37°C with 5% CO₂. Fresh serum-free RPMI media was added to the system every 3 days until they were formed to spheroid.

3. non-small cell lung cancer cell lines and cultures

The human NSCLC cell lines H460 and A549 used in this study, were obtained from the American Type Culture Collection (Manassas, VA, USA). H460 and A549 were cultured in RPMI 1640 medium and Dulbecco's Modified Eagle's Medium (DMEM) (Gibco, Grand Island, NY, USA). The culture medias were supplemented with 10% FBS (Merck, DA, Germany), 2 mM L-glutamine, and 100 units/mL of each of penicillin and streptomycin (Gibco, Grand Island, NY, USA). Cells were placed at 37 °C with 5% carbon dioxide (CO₂) in a humidified incubator.

4. Reagents and Antibodies

Roswell Park Memorial Institute (RPMI) 1640 medium, Dulbecco's Modified Eagle's Medium (DMEM), penicillin/streptomycin, L-glutamine, phosphate buffered saline (PBS), and trypsin-EDTA were obtained from Gibco (Grand Island, NY, USA). 3-(4, 5-dimethylthiazol-2-yl)-2,5-diphenyltetrazolium bromide (MTT), Propidium iodide (PI), Hoechst 33342, Triton X-100 and dimethyl sulfoxide (DMSO) were purchased from Sigma-Aldrich, Co. (St. Louis, MO, USA). Bovine serum albumin (BSA) and glycerol were obtained from Merck (DA, Germany). Fetal bovine serum (FBS) and agarose were obtained from Bio-Rad Laboratories (Hercules, CA, USA). Radioimmunoprecipitation assay (RIPA)buffer was obtained from Cell Signaling Technology, Inc. (Danvers, MA, USA). Antibodies for

CD133 (#CA1217) was obtained from Cell Applications, Inc. (San Diego, CA, USA), ALDH1A1(#36671), Nanog (#4903), Oct4 (#2750), Akt (#9272), phosphorylated Akt (#4060) and β -actin (#4970), as well as peroxidase-conjugated secondary antibodies were obtained from Cell Signaling Technology, Inc. (Danvers, MA, USA).

5. Cell Viability Assay

For cytotoxic testing, cell viability assay was performed by using the colorimetric MTT assay. NSCLC cell line (H460) was seeded onto 96 well plates at a density of 1×10^4 cells per well and incubated 24 h for cell attachment. After that, various concentrations of PME (0-500 μ M) were treated for 24 h. After treatment the RPMI media was removed and replaced with MTT solution, incubated at 37 °C for 4 h. Then removed MTT solution and added 100 μ l DMSO to dissolve the formazan crystal, measure the absorbance at 570 nm by using microplate reader (Anthros, Durham, NC, USA). The cell viability was calculated as follows:

$\% \text{ Cell viability} = (\text{optical density of treatment group} / \text{optical density of control group}) \times 100$

6. Nuclear staining assay

To evaluate apoptotic and necrotic cell death, NSCLC cell line (H460) was seeded onto 96 well plates at a density of 1×10^4 cells per well and incubated for 24 h. Then, cells were treated with PME at various concentrations (0-100 μM) and incubated for 24 h. After treatment, cells were incubated with Hoechst 33342 and propidium iodide (PI) (Sigma, St. Louis, MO, USA) 10 μM at 37 °C for 30 min. Cells were visualized and imaged under a fluorescence microscopy (Olympus DP70, Melville, NY, USA). Apoptotic and necrotic cell death were scored and analyzed as the percentages of all cells viewed.

7. Colony Formation Assay

Colony Formation Assay was used to determine the ability of cell growth in normal attachment condition (Adherent cells; anchorage dependent).

Part1; H460, A549 and patient-derived primary NSCLC cells were seeded in 6 well plates at a density of 300 cells/well and all of cells were incubated for 7 days. Culture RPMI and DMEM media (200 μl /well) was fed to the system every 3 days. After 7 days the colony was washed with PBS, fixed with 4% paraformaldehyde (Sigma Chemical, St. Louis, MO, USA) in PBS for 15 minutes, stained with 0.1% crystal violet for 30 minutes at room temperature and rinsed with PBS. Colony formation was assessed

and counted the results from three independent experiments ($n = 3$). Colony size and colony number were determined by using ImageJ 1.52v software.

Part2; NSCLC cell line (H460) was pre-treated with PME at non-toxic concentrations (0–25 μM) and incubated for 24 h at 37°C before subject to the assay. Culture RPMI media (200 μl /well) was fed to the system every 3 days. After 7 days the colony was washed with PBS, fixed with 4% paraformaldehyde (Sigma Chemical, St. Louis, MO, USA) in PBS for 15 minutes, stained with 0.1% crystal violet for 30 minutes at room temperature and rinsed with PBS. Colony formation was assessed and counted the results from three independent experiments ($n = 3$). Colony size and colony number were determined by using ImageJ 1.52v software (<http://imagej.nih.gov/ij/index.html>, Bethesda, MD, USA) with compared to the control group.



8. Anchorage independent growth assay

Anchorage-independent cell growth, property of CSCs was determined in two-layer soft agar assay.

Part1; To prepare the lower layer, using a combination of cultured media and melted 1% agarose (Bio-Rad, Hercules, CA, USA) at a 1:1 ratio, and then 500 μl of this mixture was put in a 24-well plate and allowed to solidify at 4°C for 20 minutes. To

prepare the upper layer, melted 0.3% agarose and cultured media with 10% FBS (Merck, DA, Germany) containing H460, A549 and patient-derived primary NSCLC cells at a density of 1×10^3 cells/ml and then 250 μl of this mixture was added as an upper layer. After the upper layer was solidified, the cultured RPMI media was added over the upper layer and incubated at 37°C for 2 weeks. Further cultured RPMI media (200 μl /well) was applied every 3 days to prevent the soft agar drying. Colony formation was determined after 3 weeks using a phase-contrast microscope (Nikon ECLIPSE Ts2, Tokyo, Japan). Colony number and size were counted and determined by using ImageJ 1.52v software.

Part2; NSCLC cell line (H460) was pre-treated with PME at non-toxic concentrations (0–25 μM) and incubated for 24 h at 37°C before subject to the assay. To prepare the lower layer, using a combination of RPMI media and melted 1% agarose (Bio-Rad, Hercules, CA, USA) at a 1:1 ratio, and then 500 μl of this mixture was put in a 24-well plate and allowed to solidify at 4°C for 20 minutes. To prepare the upper layer, melted 0.3% agarose and RPMI media with 10% FBS (Merck, DA, Germany) containing H460 at a density of 1×10^3 cells/ml and then 250 μl of this mixture was added as an upper layer. After the upper layer was solidified, the cultured RPMI media was added over the upper layer and incubated at 37°C for 3 weeks. Further cultured RPMI media (200 μl /well) was applied every 3 days to prevent the soft agar drying. Colony formation was determined after 3 weeks using a

phase-contrast microscope (Nikon ECLIPSE Ts2, Tokyo, Japan). Colony number and size were counted and determined by using ImageJ 1.52v software compared with the control group.

9. Spheroid formation assay

A Spheroid formation assay was performed under non-adherent and serum-free condition.

Part1; H460, A549 and patient-derived primary NSCLC cells were cultured in a 24-well ultra-low attachment plate at a density of 5×10^3 cells/ml in serum-free media and incubated at 37°C for 7 days. Fresh serum-free media was added to the system every 3 days. Primary spheroids were allowed to form and photographed at day 7 by using a phase-contrast microscope (Nikon ECLIPSE Ts2, Tokyo, Japan). Then primary spheroids were resuspended into single cell and again 5×10^3 cells/ml were cultured onto a 24-well ultralow attachment plates using serum-free media and incubated at 37°C for 14 days. Secondary spheroids were allowed to form and photographed at day 14 and 21. Characterization of CSCs populations were carried out at day 21 of spheroid culture. The spheroid number and size were analyzed by using ImageJ 1.52v software

Part2; NSCLC cell line (H460) was pre-treated with PME at non-toxic concentrations (0–25 μM) and incubated for 24 h at 37 °C before subject to the assay. H460 was cultured in a 24-well ultra-low attachment plate at a density of 5×10^3 cells/ml in serum-free RPMI media and incubated at 37°C for 7 days. Fresh serum-free RPMI media was added to the system every 3 days. Primary spheroids were allowed to form and photographed at day 7 by using a phase-contrast microscope (Nikon ECLIPSE Ts2, Tokyo, Japan). Then primary spheroids were resuspended into single cell and again 5×10^3 cells/ml were cultured onto a 24-well ultralow attachment plates using RPMI serum-free media and incubated at 37°C for 14 days. Secondary spheroids were allowed to form and photographed at day 14 and day 21. Characterization of CSCs populations were carried out at day 21 of spheroid culture. The spheroid number and size were analyzed compared with the control group.

After patient-derived primary NSCLC were allowed to grow as spheroids. The spheroids were treated with a non-cytotoxic concentration of PME (0–25 μM). The images of the spheroids were taken at day 0 and day 7 after PME treatment under a phase-contrast microscope (Nikon ECLIPSE Ts2, Tokyo, Japan). The spheroid size was analyzed compared with the control group.

10. Western blot Analysis

Levels of protein expression were evaluated using Western blot analysis. NSCLC cell line (H460) was seeded at a density of 5×10^5 cells/well overnight. The cells were lysed using lysis buffer containing RIPA buffer, 1% Triton X-100, 100 mM PMSF and a protease inhibitor for 45 minutes on ice bath. The cell lysates were collected and protein content was measured by using BCA protein assay kit from Pierce Biotechnology (Rockford, IL). An equal amounts of denatured protein samples (60 μ g) were separated onto 10% sodium dodecyl sulfate polyacrylamide gel electrophoresis (SDS-PAGE) and transferred polyvinylidene difluoride (PVDF) (Bio-Rad Laboratories Inc., CA, USA). Transferred membranes were blocked for at least 30 min with 5% nonfat-milk in Tris-buffered saline solution containing 1% Tween-20 (TBST) and then incubated with the indicated primary antibody against CD133 (Cell Applications, San Diego, CA, USA), ALDH1A1, Nanog, Oct4, Akt, phosphorylated Akt and β -actin (Cell Signaling, Danvers, MA, USA) at 4°C overnight. Thereafter, the membranes were washed 3 times with TBST for 10 minutes and incubated with secondary antibody at room temperature for 2 h. After 3 washes with TBST, the antigen-antibody complexes were detected by enhancement with chemiluminescent solution (Supersignal West Pico; Pierce, Rockford, IL, USA) and quantified the proteins expression levels using ImageJ 1.52v software.

11. Immunofluorescence Assay

NSCLC cell line (H460) and patient-derived primary NSCLC cells were seeded at a density of 1×10^4 cells/well in 96-well plates and incubated overnight. The cells were treated with PME for 24 h. After treatment, the cells were washed with $1 \times$ PBS and fixed with 4% paraformaldehyde for 20 min and permeabilized with 0.1% Triton-x in PBS for 20 min. Then, blocked with 4% BSA in $1 \times$ PBS for 30 min at room temperature, washed and incubated with primary antibody (selected from western blot analysis results) overnight at $4 \text{ }^\circ\text{C}$, washed with $1 \times$ PBS and incubated with secondary antibodies for 1 h at room temperature in the dark. After that, the cell was washed with PBS, and incubated with Hoechst 33342 (Sigma, St. Louis, MO, USA) for 20 min in the dark, rinsed with $1 \times$ PBS and mounted by 50% glycerol (Merck, DA, Germany). Visualized and imaged using fluorescence microscopy with a $40 \times$ objective lens (Nikon ECLIPSE Ts2, Tokyo, Japan) and the analysis was assessed by ImageJ software.

12. Protein and Ligands Preparation

The protein structure of the Akt-1 complexed with the ligand inhibitor (CQW) was downloaded from the Research Collaboratory for Structural Bioinformatics Protein Data Bank (RCSB PDB) (126) at 2 \AA (PDB ID: 3CQW) (127). Before docking simulation, all water molecules and ligand were removed with the UCSF ChimeraX

(128). Hydrogen atoms added with the program reduce (129) in AutoDockFR (130). The 3D structure of CQW was extracted from 3CQW PDB code and used as a reference. The 3D structure of PME was download from the PubChem database (131) (Pubchem CID: 636768). The gaussian 09 program (132) applied to optimize the geometry of the ligands using density functional theory (DFT) with a B3LYP/6-31G(d,p) basis set. These ligand structures are illustrated in Figure 18a.

13. Molecular Docking

In the molecular docking simulation, AutoDock vina (133) was employed to clarify both binding mode and affinity of the selected potential Akt-1 inhibitor. A grid box was set with the centre of the co-crystallized ligand inhibitor (CQW of 3CQW) and dimension ($x = 20$, $y = 20$, and $z = 20$), with a spacing of 1 \AA (134). The exhaustiveness parameter was set to 24 (135). Other AutoDock vina parameters were set as default. The binding pattern of protein–ligand interaction was analysed using the UCSF ChimeraX.

14. Bioinformatics Analysis; PPI Networks Integration and KEGG Pathway Maps Analyses

To identify the interaction between the CSC marker proteins that affected by PME treatment, the PPI networks were construct using STITCH (<http://stitch.embl.de/>; version 5.0/accessed on 23 July 2021) online database. After that, the CSC marker proteins were also encoded to the network-based classification of KEGG Ontology (KO) as follows: Akt (K04456), Oct4 (K09367), Nanog (K10164), CD133 (K06532) and ALDH1A1 (K07249) before analysis. KEGG pathway maps analysis and functional annotation for the selected encoded proteins were performed by utilizing involved signaling pathways associated with CSCs (<https://www.genome.jp/kegg>, accessed on 23 July 2021).

15. Statistical analysis

The data from three independent experiments (n = 3) was presented as the mean \pm standard error of the mean (S.E.M.). Statistical differences between multiple groups were analyzed using an analysis of variance (ANOVA), followed by individual comparisons with Bonferroni's post-hoc test. The p-value of less than 0.05 was considered as statistically significant.

16. Ethical Consideration

Thai non-small cell lung cancer patients with malignant pleural effusion who had been diagnosed and receiving treatment at the King Chulalongkorn Memorial Hospital, were prospectively enrolled in the study. Informed consent was obtained from all patients and this study was approved by the Ethics Committee of the Faculty of Medicine, Chulalongkorn University, Bangkok, Thailand (Institutional Review Board; IRB 365/62) (Date of Approval: 31 July 2020). The malignant pleural effusion was collected from a part of standard diagnosis practice and clinical treatment.



Conceptual framework

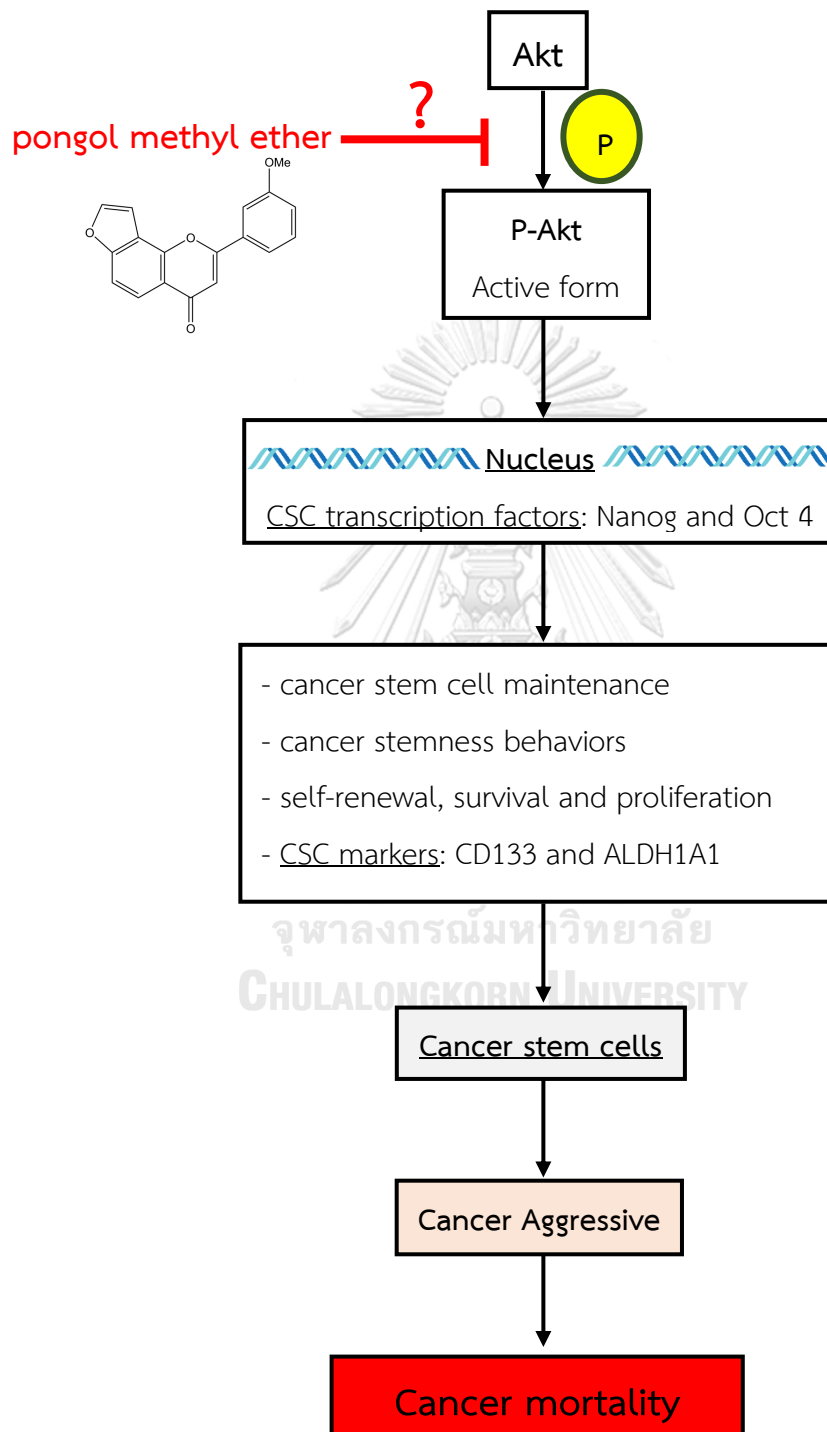


Figure 2 Conceptual framework of this study

Research design

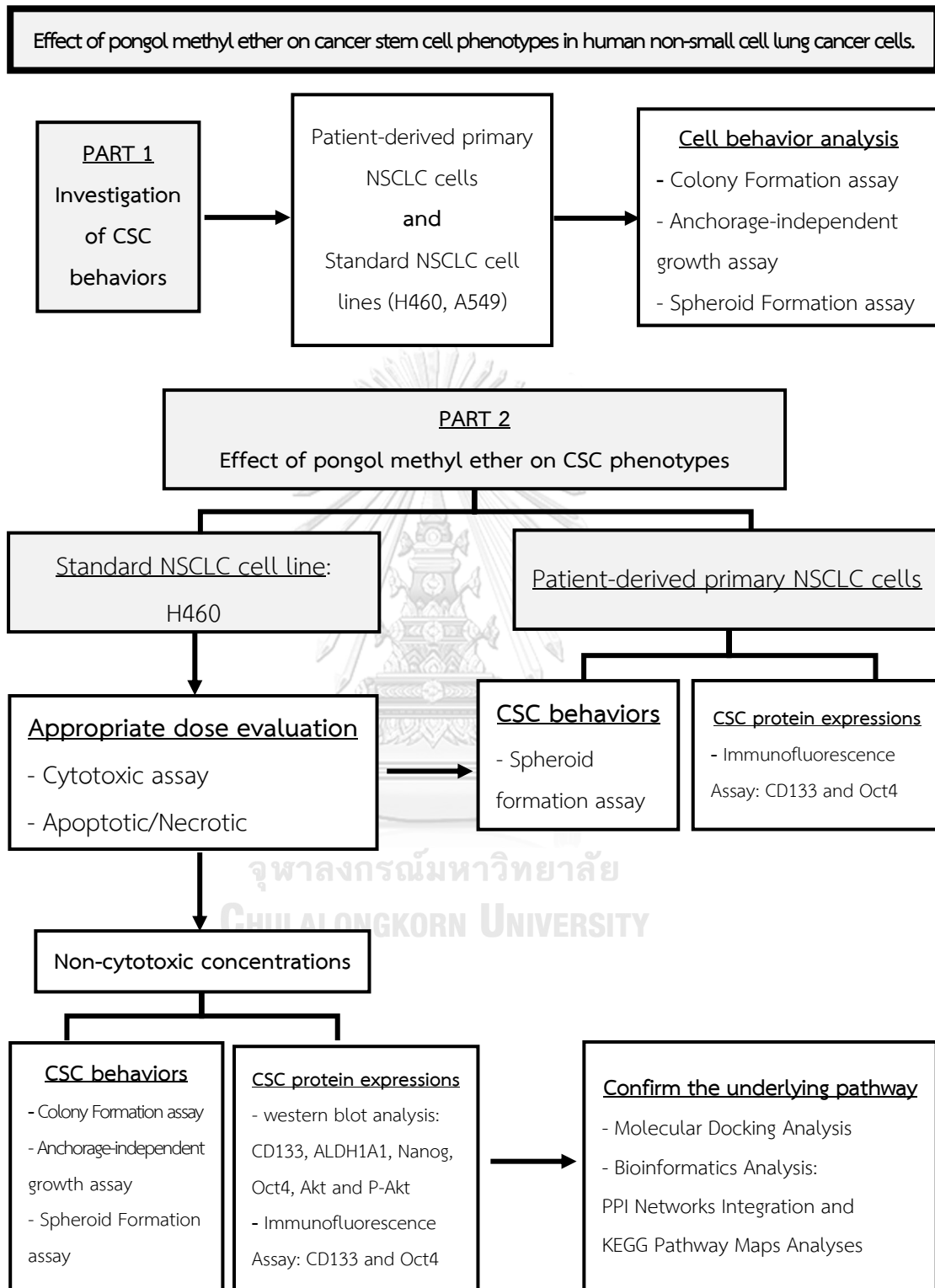


Figure 3 Research design of this study

Administration and time schedule

Activities	1st year		2nd year	
	1st semester	2nd semester	1st semester	2nd semester
Literature review				
Laboratory skill practice				
Research planning				
Equipment preparation				
Data collection				
Data analysis				
Academic report and publication				

จุฬาลงกรณ์มหาวิทยาลัย
CHULALONGKORN UNIVERSITY

Table 3 Administration and time schedule

Budget

	Baht
Lung cancer cells	150,000
Cell culture equipment	
- pipette tips	7,000
- Eppendorf tube	3,000
- culture plates (6, 24, 96 well)	10,000
- 15 and 50 ml conical tube	5,000
- Chemicals	
- RPMI media	15,000
- fetal bovine serum (FBS)	10,000
- penicillin-streptomycin	2,500
- trypsin-EDTA	2,500
- Hoechst 33342	10,000
- Propidium iodide	10,000
- western blot assay	
- MTT assay	50,000
- Antibody	10,000
- Miscellaneous	100,000
Total	385,000

Table 4 Budget

CHAPTER IV

RESULTS

Part 1 Investigation of CSC behaviors

1. Cell behavior analysis: Colony Formation assay

Colony formation assay was used to determine the ability of cell proliferation in normal attachment condition (Adherent cells; anchorage dependent). H460, A549 and patient-derived primary NSCLC cells were seeded and incubated for 7 days. The cells were fixed and stained with 0.1% crystal violet. Colony number and size were assessed and counted after 7 days.

Figure 4 showed that human lung cancer cell lines, H460 and A549 were highly capable to forming colony numbers more than patient-derived primary NSCLC cells. H460 has the highest number of colonies, while the highest number of patient-derived primary NSCLC cells group was ELC08 significantly. In term of the colony size, has not more different of such cells and ELC17 was the significant lowest in size than the others as well as colony number.

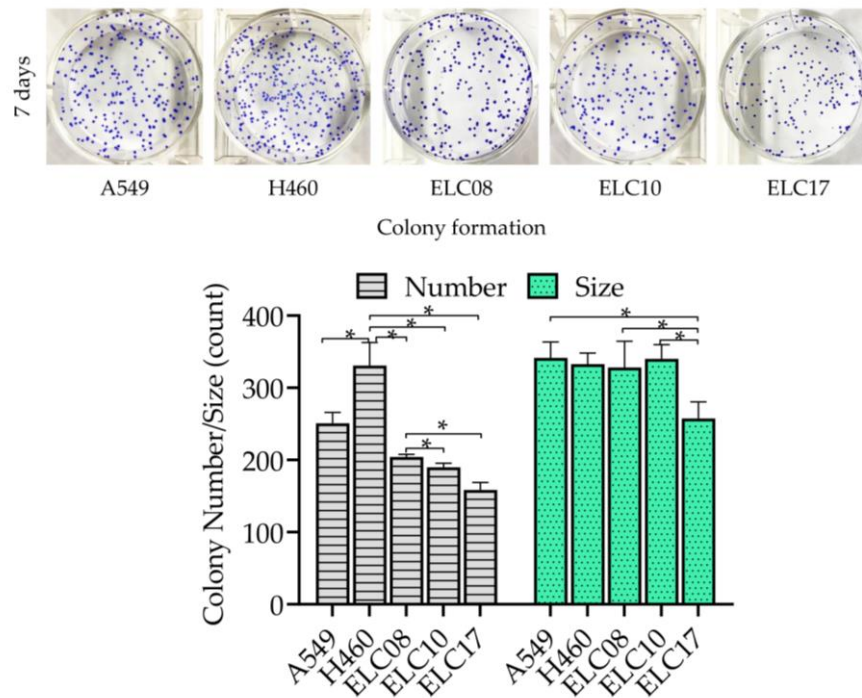


Figure 4 Colony Formation assay

Cells were seeded, incubated and colonies were stained by crystal violet after 7 days. Data are presented as the mean \pm SEM ($n = 3$). The asterisk (*) indicates a significant difference ($p < 0.05$).

2. Cell behavior analysis: Anchorage-independent growth assay

An anchorage-independent growth assay was used as a behavioral analysis that reflects the self-renewal, anoikis resistance and tumorigenic capability of CSCs (136). The CSC properties of H460, A549 and patient-derived primary NSCLC cells were determined in a two-layer soft agar assay. Colony formation was determined after 3 weeks.

Figure 5 indicated that H460 has significant highest ability to generating colony numbers than other cells, while ELC08 had the significant highest colony numbers compared in patient-derived primary NSCLC cells group at both of day 14 and 21 respectively. In term of colony size, A549 cell line had shown highest ability to form the size of colony bigger than H460 and ELC08 significantly, whereas ELC10 had the second highest colony size at both of day 14 and 21 respectively.

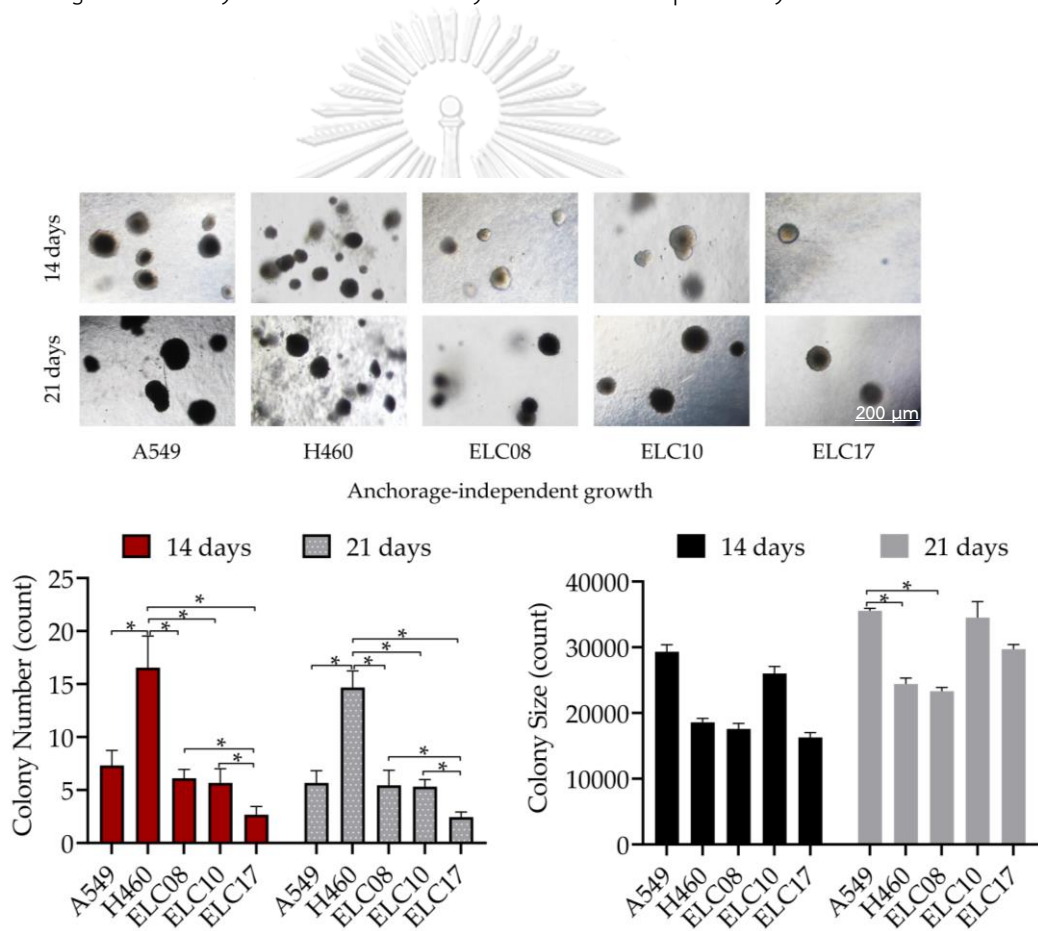


Figure 5 Anchorage-independent growth.

Cells were subjected to two-layer soft agar assay. Colony number and size were evaluated after day 14 and 21. Data are presented as the mean \pm SEM (n = 3). The asterisk (*) indicate a significant (p < 0.05).

3. Cell behavior analysis: Spheroid formation assay

Self-renewal and tumorigenicity are a hallmark of CSCs. These abilities could induce CSCs to form spheroids as well as growth and survival in anchorage-independent condition (7) (137). A Spheroid formation assay was performed under non-adherent and serum-free condition. H460, A549 and patient-derived primary NSCLC cells were cultured and incubated for 21 days. Primary spheroids and secondary spheroids were allowed to form and photographed at day 7, 14 and 21.

In term of primary spheroids, H460 had shown to generate the highest primary spheroid numbers and A549 has the highest primary spheroid size, significantly. In addition, ELC10 has the highest primary spheroid numbers and ELC17 had shown the significant highest of primary spheroid size when compared in the patient-derived primary NSCLC cells group (figure 6).

The secondary spheroids are a number of spheroids that remain in such condition after resuspended primary spheroids, indicating to an existence of CSC capabilities (138) (139). Figure 7 revealed that H460 has highest ability to generating spheroid numbers than other cells, while ELC08 has the highest spheroid numbers compared in patient-derived primary NSCLC cells group at both of day 14 and 21 significantly. In term of spheroids size, A549 cell line had shown highest ability to form the size of spheroid bigger than ELC08 and ELC17 significantly, whereas ELC10

had shown the significant highest of spheroid size compared in patient-derived primary NSCLC cells group at both of day 14 and 21.

Taken together, the results from part 1 revealed that H460 cells as the most aggressive cells and exhibited the highest CSC phenotypes with highly numbers of colony and spheroid formation. Having demonstrated the highest CSCs-behavioral cells from all human NSCLC cell samples group. We next investigated the CSCs-suppressing effects of PME in human NSCLC cells using H460 as the selected representative cell.

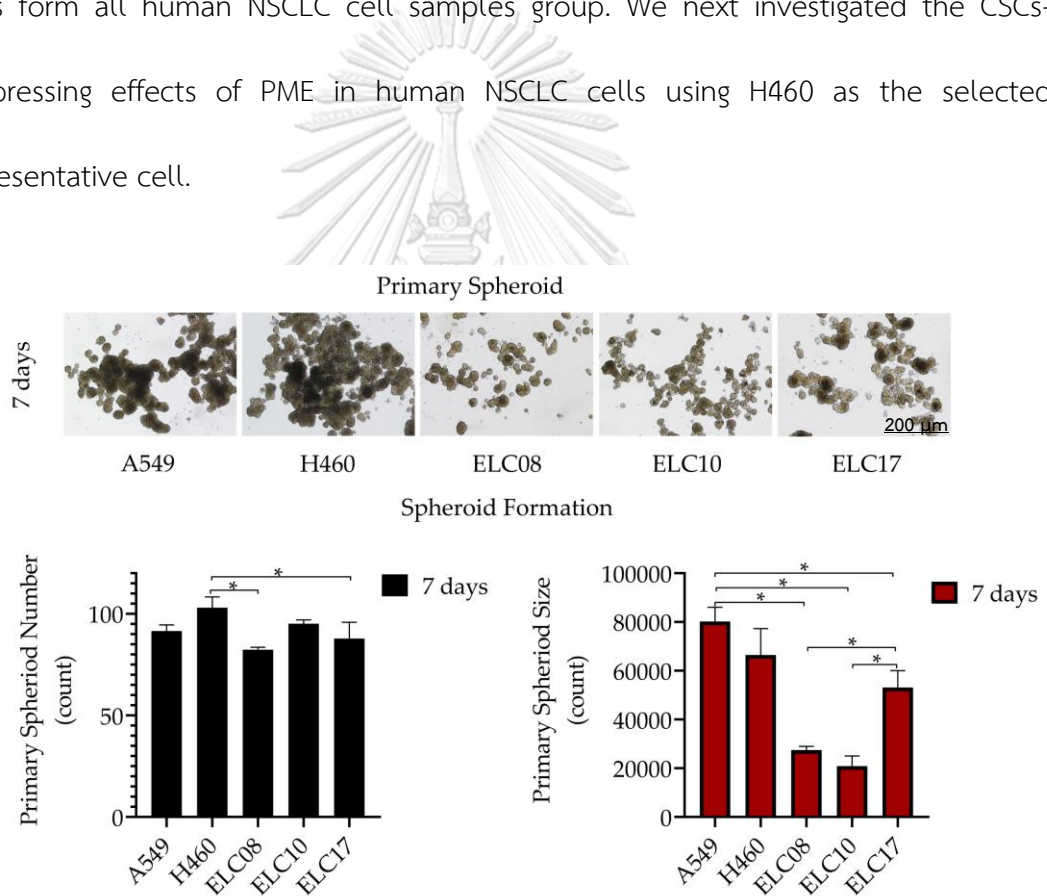


Figure 6 Primary spheroids.

Cells were subjected to spheroid formation assay. Primary spheroids were captured under microscopic with 4x magnification. The spheroid size and number were quantified. Data are presented as the mean \pm SEM (n = 3). The asterisk (*) indicate a significant (p < 0.05).

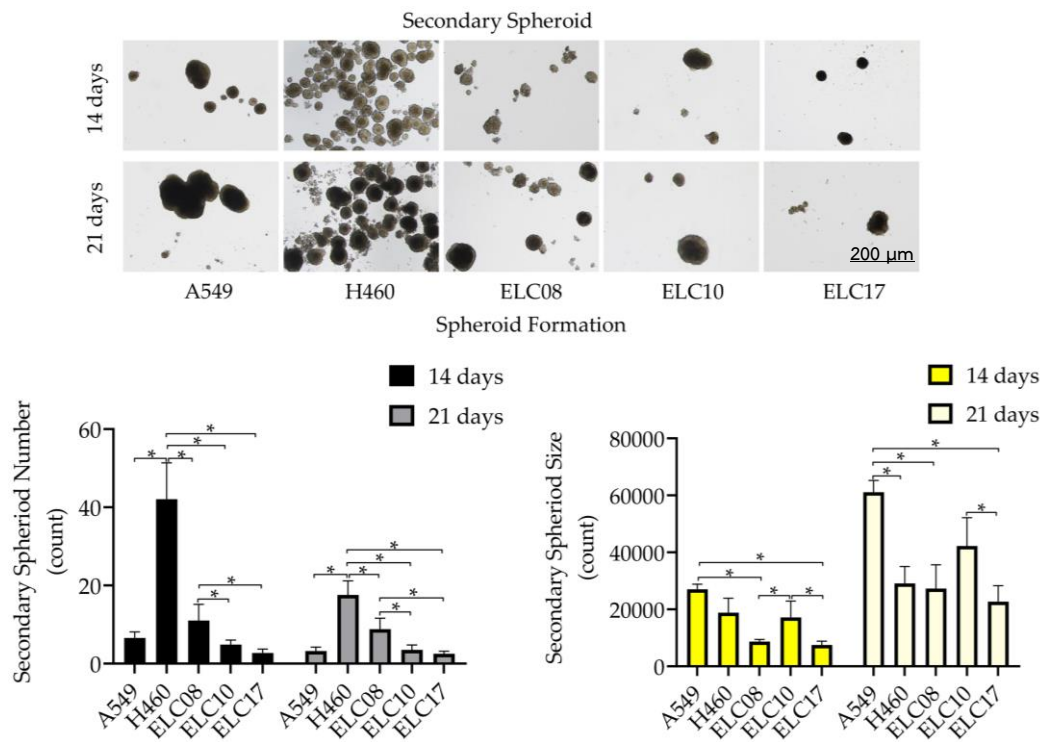


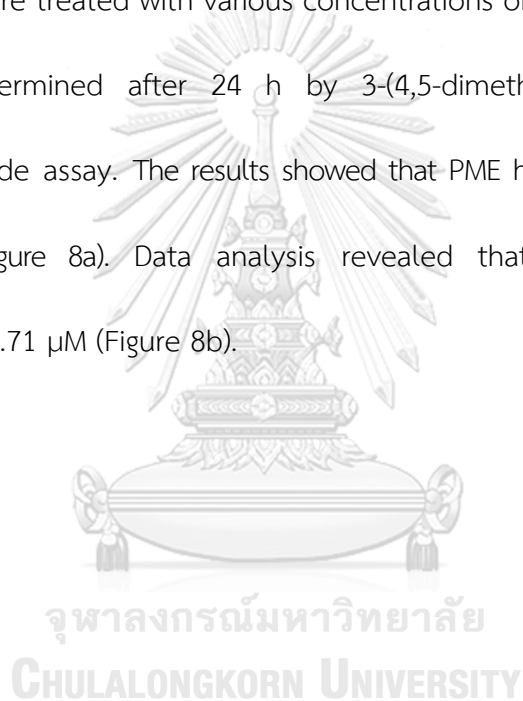
Figure 7 Secondary spheroids.

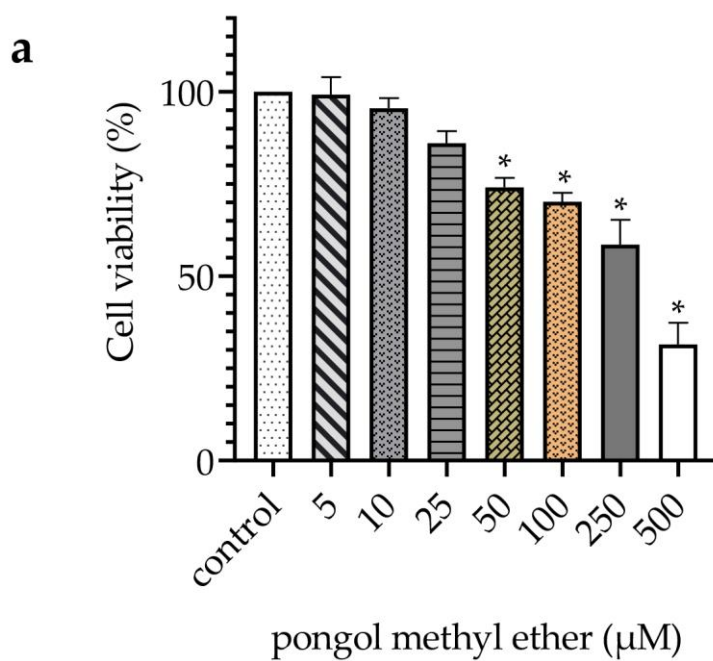
The primary spheroids were resuspended into single cells to form secondary spheroids. After 14 and 21 days the secondary spheroids number and size were determined. Data are presented as the mean \pm SEM (n = 3). The asterisk (*) indicate a significant ($p < 0.05$).

Part 2 Effect of pongol methyl ether on CSC phenotypes

1. Cytotoxicity and Anti-Proliferative Effect of PME on H460 Lung Cancer Cells.

To diminish the interference from the cytotoxic effect of PME on CSC phenotypes, we first evaluated the non-cytotoxic concentrations of PME on H460 cells. The cells were treated with various concentrations of PME (0–500 μM), and cell viability was determined after 24 h by 3-(4,5-dimethylthiazol-2-yl)-2,5-diphenyl tetrazolium bromide assay. The results showed that PME has non-toxic concentrations below 50 μM (Figure 8a). Data analysis revealed that the IC_{50} of PME was approximately 327.71 μM (Figure 8b).





b

Cell	IC ₅₀ ± SEM (μM)
H460	327.71 ± 22.11

Figure 8 Cytotoxic effect of PME.

(a) H460 cells were treated with PME at various concentrations (0–500 μM) for 24 h, and cell viability was measured. (b) IC₅₀ of H460 cells at 24 h of PME treatment. Data are presented as the mean ± SEM (n = 3). * p < 0.05 compared with nontreated cells.

Hoechst 33342 and propidium iodide nuclear staining assay indicated that the PME treatment at 0–25 μM had no significant effect on the apoptosis or necrosis of cells. The significant increase in apoptosis was observed when the cells treated with PME at 50 and 100 μM showed approximately 5% and 10% increase in apoptotic cell death, respectively (Figure 9).

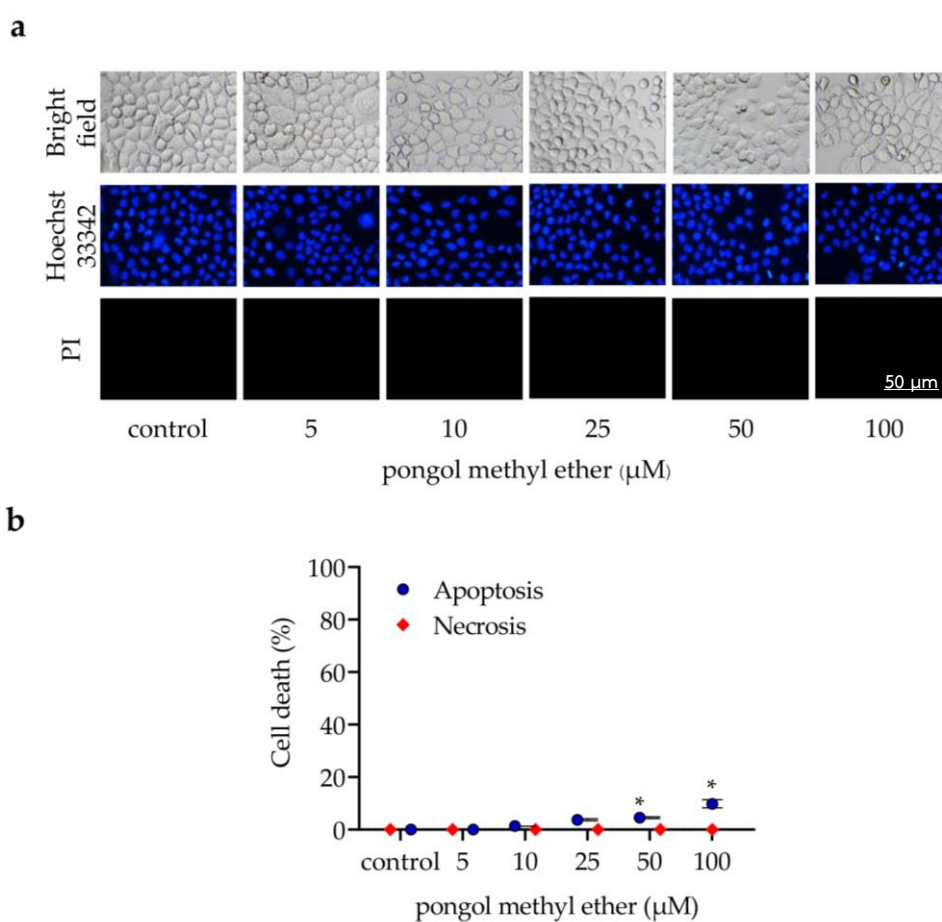


Figure 9 Apoptosis effect of PME on H460 cells.

Apoptotic and necrotic cell death were evaluated by Hoechst 33342/PI staining and calculated as a percentage compared with non-treated control cells. Data are presented as the mean \pm SEM (n = 3). * p < 0.05 compared with nontreated cells.

We also confirmed the effect of PME on cell proliferation by colony formation assay, and the results showed that PME at 5–25 μM can significantly decrease the size of colonies (Figure 10).

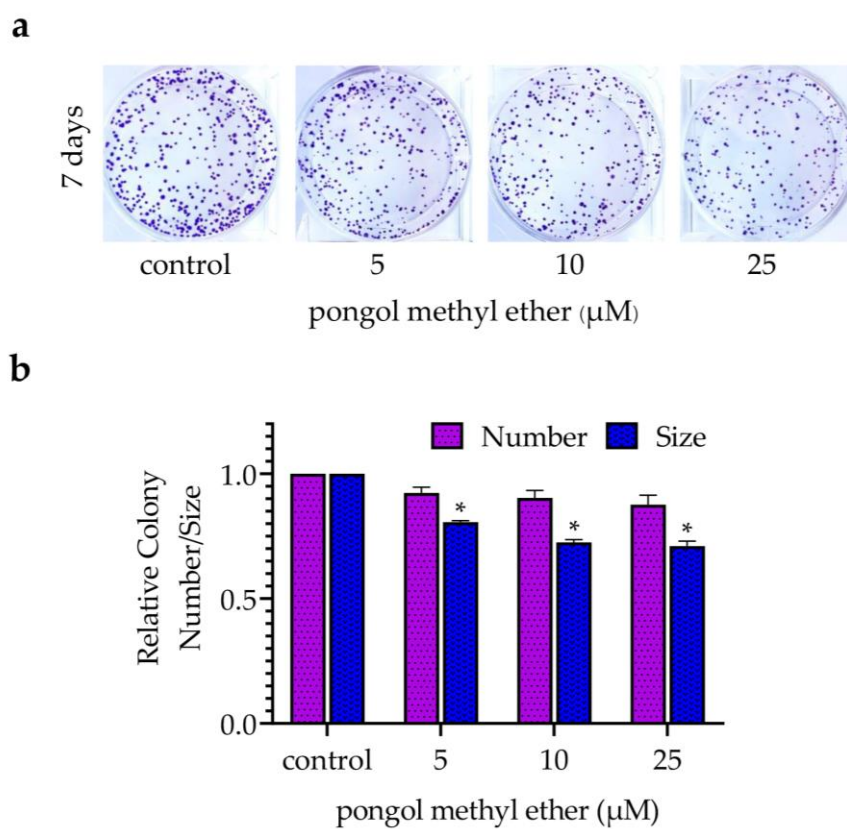


Figure 10 Effect of PME on cell proliferation by colony formation assay in H460 cells.

Cells were treated with PME at non-toxic concentrations (0–25 μM), and colony was stained by crystal violet after 7 days. Data are presented as the mean \pm SEM (n = 3). * p < 0.05 compared with nontreated cells.

2. PME Attenuates CSC Phenotypes during Anchorage-Independent Growth and Spheroid Formation.

CSCs can form spheroids and grow in an anchorage-independent condition (137) (93). Cells were pre-treated with PME (0–25 μM) for 24 h, followed by examination of their anchorage-independent growth and spheroid formation. For anchorage-independent growth, the colony number and size were determined and are presented as relative values in comparison with those of non-treated control. Figure 11a reveals that PME significantly decreased the colony number and size in a concentration-dependent manner. A significant suppression of colony growth was first detected at 5 μM PME, with approximately 25 and 30% reduction in the colony number and size at 14 days, respectively (Figure 11b). Moreover, PME at 25 μM can reduce 65 and 70% of the colony number and size, respectively, at 21 days (Figure 11c).

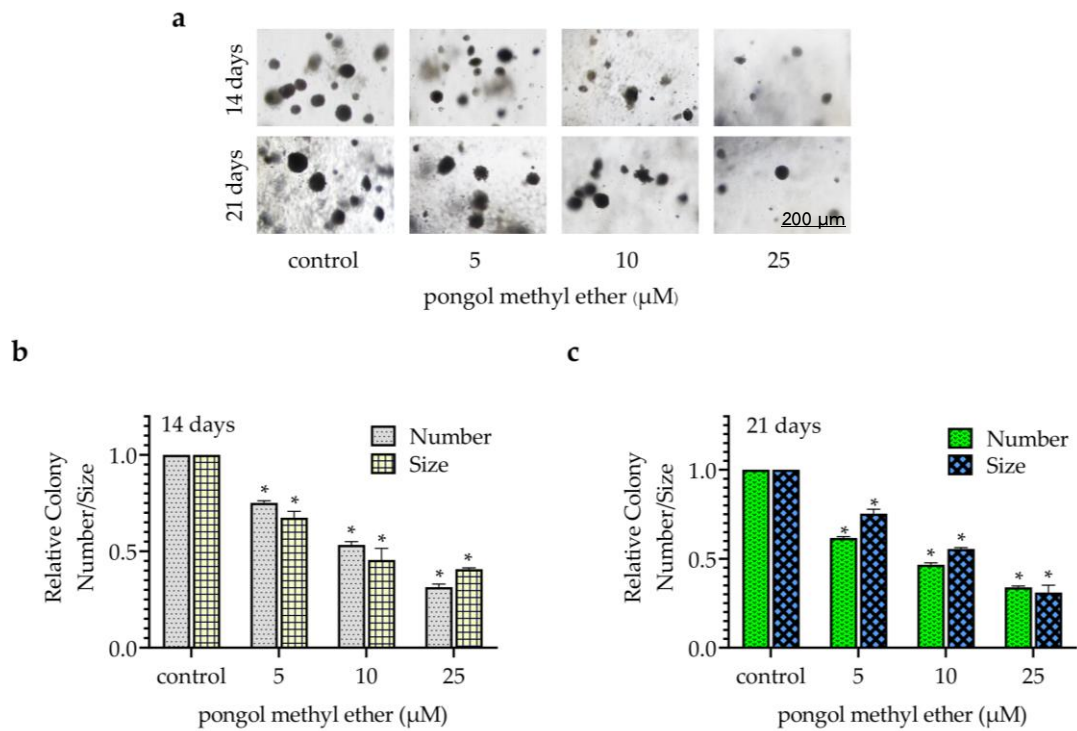
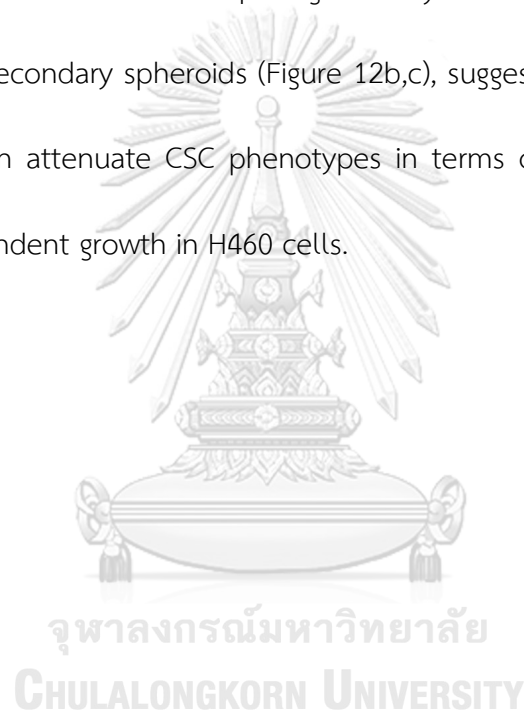


Figure 11 PME suppresses anchorage-independent growth.

(a) H460 cells were pre-treated with PME (0–25 μM) for 24 h and subjected to an anchorage-independent growth assay. (b,c) Colony number and size were evaluated after day 14 and 21.

Data are represented as mean \pm SEM ($n = 3$) * $p < 0.05$ compared with untreated cells.

For spheroid formation, the cells were pre-treated with PME (0–25 μM) for 24 h. Then, the cells were detached, re-suspended and seeded at a low density onto ultralow attachment plates. The non-treated cells formed spheroids, whereas the cells treated with PME exhibited a significant reduction in spheroids in a concentration-dependent manner (Figure 12a). Interestingly, the treatment of cells with PME at concentrations of 5–25 μM significantly reduced the number and size in the primary and secondary spheroids (Figure 12b,c), suggesting that PME at non-toxic concentrations can attenuate CSC phenotypes in terms of spheroid formation and anchorage-independent growth in H460 cells.



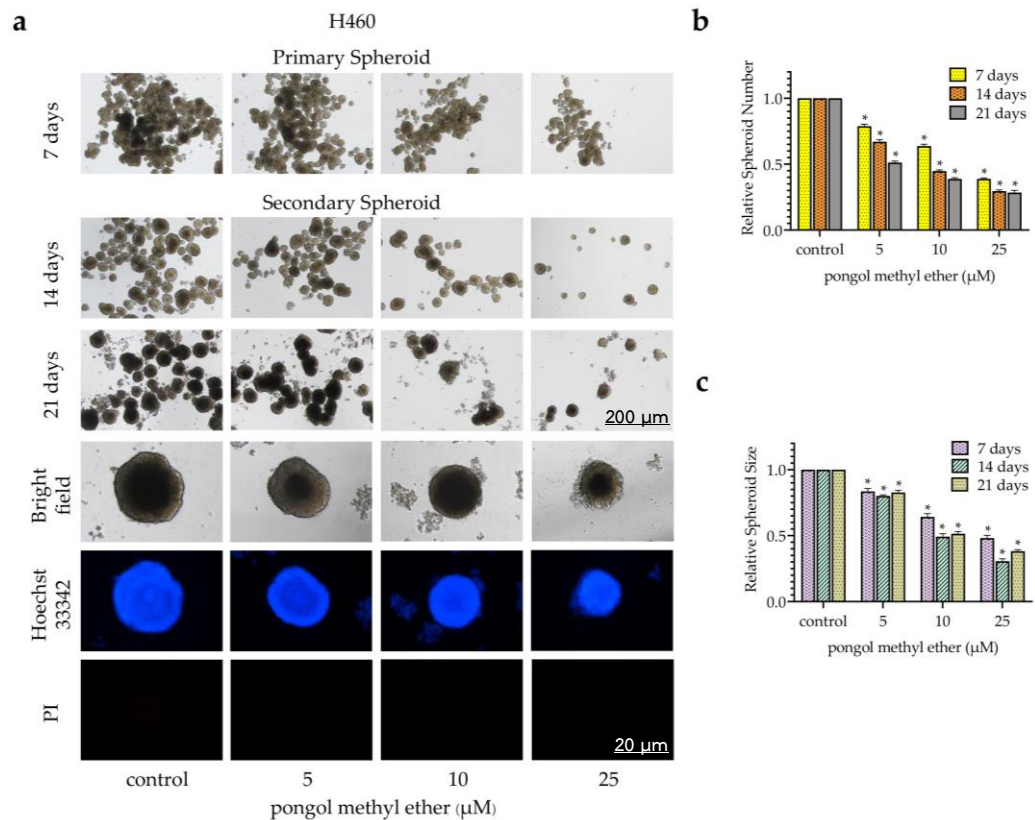


Figure 12 PME suppresses CSC-spheroid formation in H460 cells.

(a) H460 cells were treated with PME (0–25 μM) for 24 h and subjected to spheroid formation assay. (b,c) The spheroid number and size were analyzed and presented as the relative value to the control cells of each condition. Data are represented as mean \pm SEM (n = 3) * p < 0.05 compared with untreated cells.

Having demonstrated the CSC-suppressing effects of this compound in human NSCLC cell line, we next investigated whether PME can attenuate the CSC phenotypes in patient-derived NSCLC cells. CSC spheroids of patient-derived NSCLC cells were treated with non-toxic concentrations of PME (0–25 μ M). The results indicated that PME significantly reduced the ability of such cells to form spheroids compared with the control (Figure 13a–c)



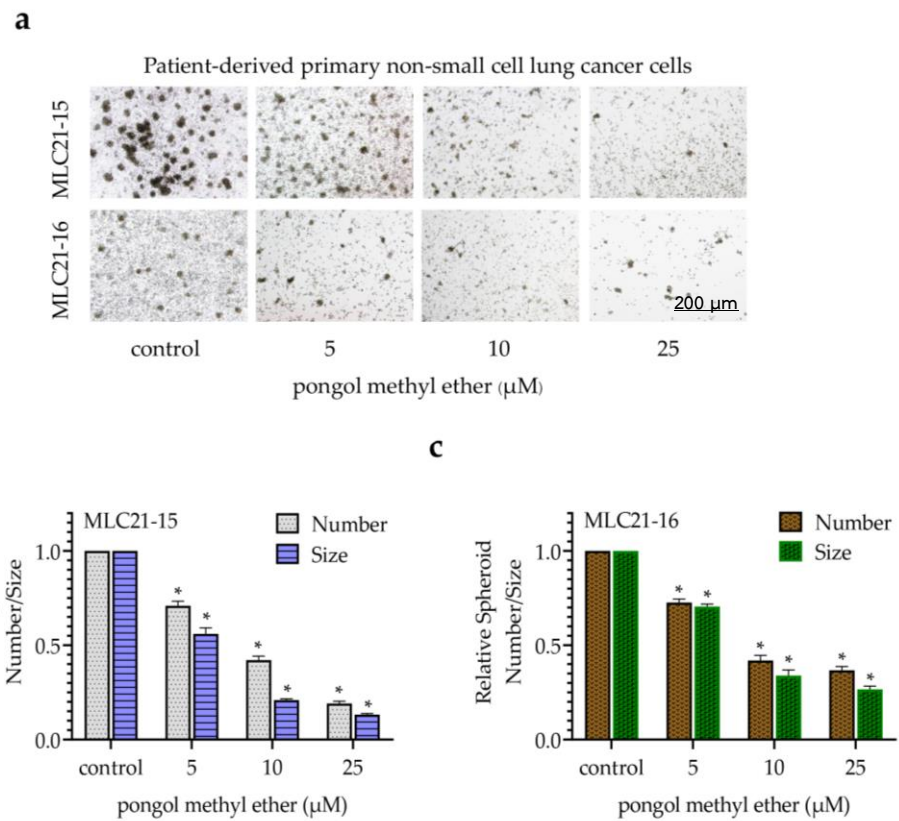


Figure 13 PME suppresses CSC-spheroid formation in patient-derived NSCLC cells.

(a) CSC-spheroids of patient-derived NSCLC cells were treated with PME (0–25 μM). (b,c) After 7 days, the spheroid number and size were determined. Data are represented as mean \pm SEM (n = 3) * p < 0.05 compared with untreated cells.

3. PME Reduces CSC Markers and Pluripotent Transcription Factors through the Reduction of the Akt Signaling Pathway.

Next, the expression of CSC-specific markers in the cells in response to PME were investigated. H460 cells were incubated with PME (0–25 μM) for 24 h, and the expression levels of CD133 and ALDH1A1 were determined by Western blot analysis. Figure 14a,b show that the treatment of cells with PME significantly reduced CD133 expression at 10 μM , whereas ALDH1A1 was reduced at 25 μM , respectively. The activated Akt controls the survival, growth and self-renewal abilities of CSCs (25). In addition, Akt induces CSC phenotypes through the upregulation of Oct4 and Nanog (27) (28). The expression levels of phosphorylated Akt, total Akt, Oct4 and Nanog were evaluated by Western blotting. Figure 14a,c reveal that PME reduced the level of phosphorylated Akt. Similarly, the stem-cell transcription factors Oct4 and Nanog significantly decreased during PME treatment at concentrations 10 and 25 μM , respectively (Figure 14a,b). Altogether, our results suggest that PME suppressed the CSC phenotypes through Akt inhibition and depleted the stem-cell transcription factors.

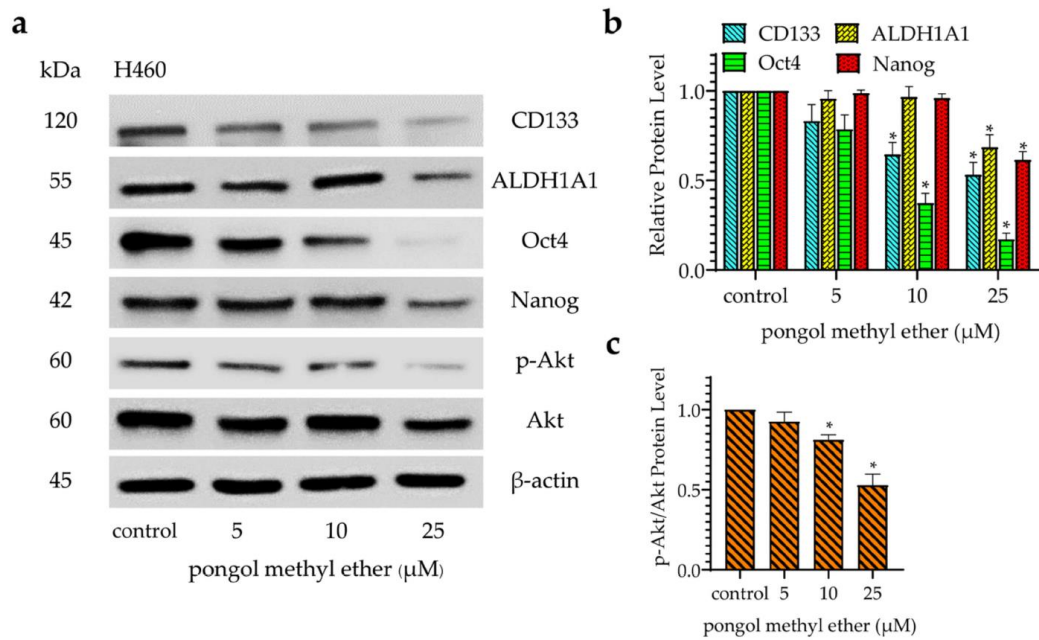


Figure 14 PME reduces CSC markers and transcription factors through inhibition of the ATP-dependent tyrosine kinase (Akt) signaling pathway.

(a) H460 cells were treated with PME (0–25 μM) for 24 h, the levels of CD133, ALDH1A1, Oct4, Nanog, phosphorylated Akt and total Akt were examined by Western blotting. The blots were re-probed with antibody against β -actin. (b,c) Relative protein levels were quantified by densitometric analysis using ImageJ. Values are means \pm SEM calculated as relative values to the non-treated control value. Data are represented as mean \pm SEM (n = 3). * p < 0.05 compared with untreated cells.

The PME depletion effects on CD133 and Oct4 were confirmed by immunofluorescence staining. Figure 15 show that PME significantly decreased the levels of CD133 and Oct4 in H460 cells.

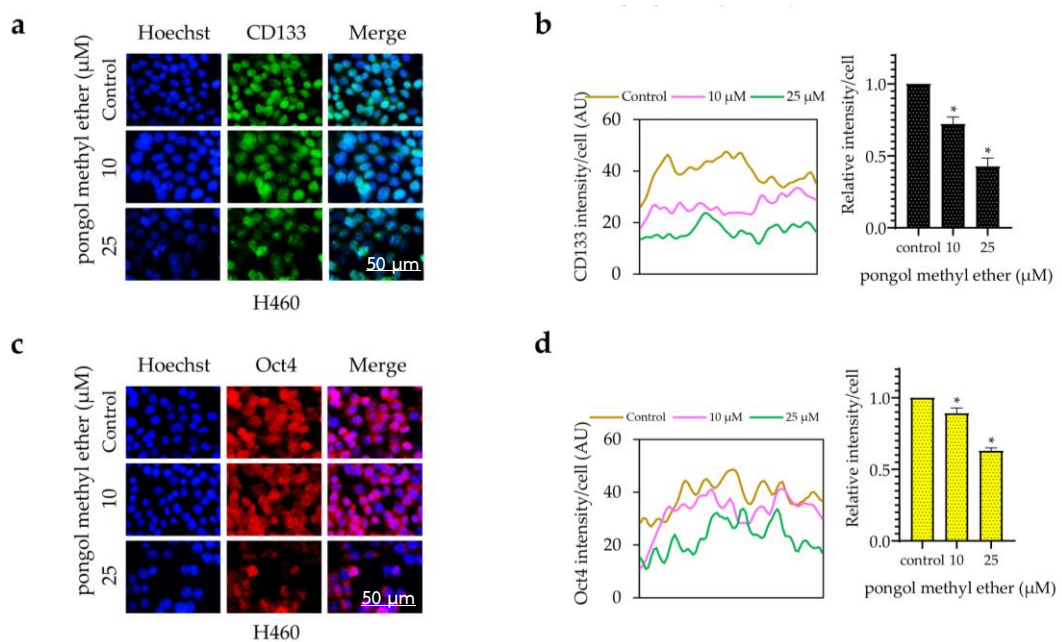


Figure 15 PME suppresses CSC marker (CD133) and transcription factor (Oct4) in H460 cells.

(a) H460 cells were treated with PME (0, 10, 25 μM) for 24 h. The cells were co-stained with anti-CD133 antibodies and Hoechst 33342. (b) The expression of CD133 was examined using immunofluorescence. (c) The cells were co-stained with anti-Oct4 antibodies and Hoechst 33342. (d) The expression of Oct4 was examined using immunofluorescence. The fluorescence intensity was analyzed by ImageJ software. Values are means ± SEM calculated as relative values to the non-treated control value. Data are represented as mean ± SEM (n = 3). * p < 0.05 compared with untreated cells.

Persistently, similar results from the immunofluorescence analysis were found in patient-derived NSCLC cells (Figure 16,17). These results showed that PME attenuated the CSC phenotypes and suppressed CSC makers and transcription factors *via* the inhibition of the Akt signaling pathway in human NSCLC cells.

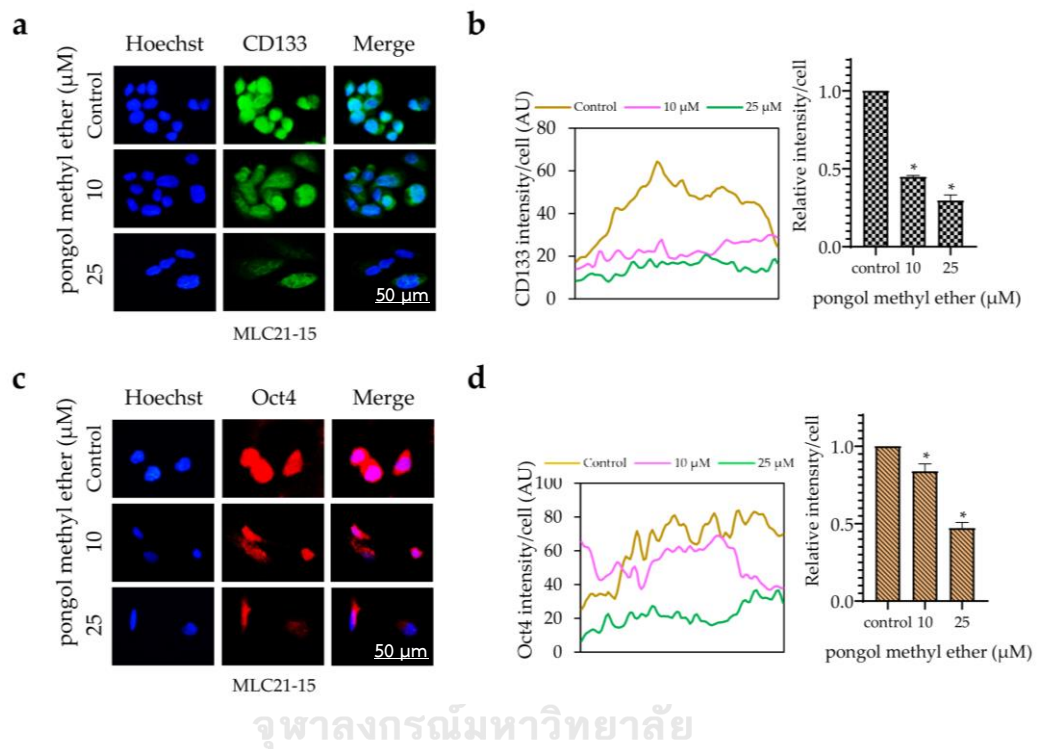


Figure 16 PME suppresses CSC marker (CD133) and transcription factor (Oct4) in patient-derived NSCLC cells (MLC21-15).

MLC21-15 was treated with non-toxic concentrations of PME (0, 10, 25 μM) for 24 h. The cells were co-stained with anti-CD133 antibodies (a); anti-Oct4 antibodies (c) and Hoechst 33342. The expression of CD133 (b) and Oct4 (d) were examined using immunofluorescence. The fluorescence intensity was analyzed by ImageJ software. Values represent the mean \pm SEM. (n = 3). * p < 0.05 compared with untreated cells.

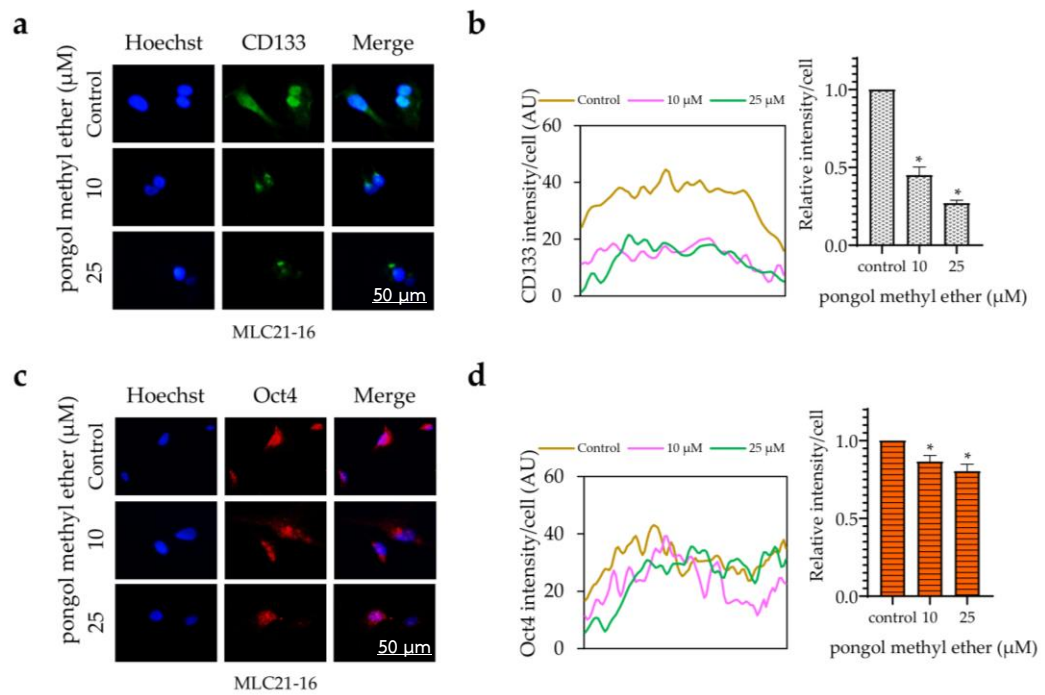


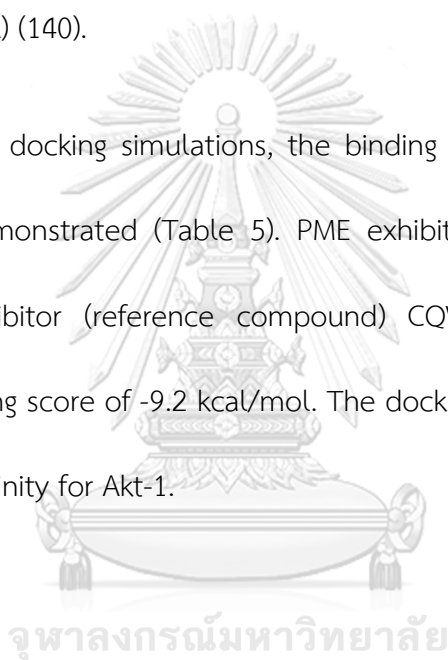
Figure 17 PME suppresses CSC marker (CD133) and transcription factor (Oct4) in patient-derived NSCLC cells (MLC21-16).

MLC21-16 was treated with non-toxic concentrations of PME (0, 10, 25 μM) for 24 h. The cells were co-stained with anti-CD133 antibodies (a); anti-Oct4 antibodies (c) and Hoechst 33342. The expression of CD133 (b) and Oct4 (d) were examined using immunofluorescence. The fluorescence intensity was analyzed by ImageJ software. Values represent the mean ± SEM. (n = 3). * p < 0.05 compared with untreated cells.

4. Molecular Docking Simulations Indicated the PME Interaction with the Akt-1 Protein.

To validate the docking protocol, we redocked CQW into its original binding site of Akt-1 (PDB ID: 3CQW). The root mean square deviation (RMSD) of the redocked ligand was 1.381 Å. The results (Figure 18b) indicate that the docking protocol was accurate (RMSD < 2 Å) (140).

In the molecular docking simulations, the binding free energy (kcal/mol) of all compounds was demonstrated (Table 5). PME exhibited a greater binding affinity than the Akt-1 inhibitor (reference compound) CQW (-8.3 kcal/mol), with an AutoDock Vina docking score of -9.2 kcal/mol. The docking results indicated that PME has a high binding affinity for Akt-1.



No.	Compounds	Free Energy of Binding (kcal/mol)
1	Pongol methyl ether	-9.2
2	(CQW) reference compound	-8.3

Table 5 Binding free energy of the docking simulations (kcal/mol)

Figure 18c,d illustrate the interaction of all compounds. The docking result of PME revealed that it contributed to the hydrophobic interactions with Leu156, Gly162, Val164, Ala177, Met218 and Met227, and formed hydrogen bonds with Lys179 and Ala230. These results suggest that PME interacted in the ATP-binding site of Akt-1, which is similar to the binding site of the reference compound.

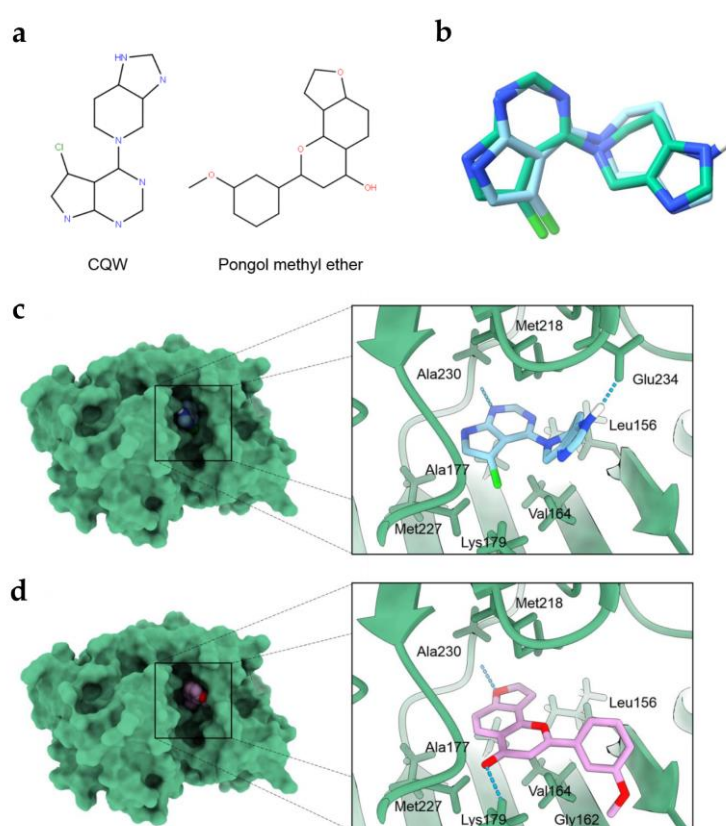


Figure 18 Molecular Docking Simulations

(a) The structure of CQW and PME. (b) Redocking of CQW in Akt-1 (PDB ID: 3CQW); CQW from the crystal (green) and CQW generated by redocking (blue). Docking interaction profile of Akt-1 inhibitors: (c) Akt-1 in complexed with CQW (reference compound), (d) Akt-1 in complexed with PME. The blue dashed lines represent hydrogen-bonding interaction.

5. Bioinformatic Analysis of the CSC Marker Proteins in PME Treatment.

Having revealed the proteins involving in PME suppression of CSC in lung cancer cells, we next aimed at investigating the dominant protein form all detected protein using bioinformatic tool. The protein–protein interaction (PPI) networks and Kyoto Encyclopedia of Genes and Genomes (KEGG) pathway maps were used to construct the interaction of the CSC marker proteins in PME treatment. Search Tool for Interactions of Chemicals (STITCH) Version 5.0 (<http://stitch.embl.de>, accessed on 23 July 2021) was employed to identify the binding partners for NANOG, POU5F1 (POU class 5 homeobox 1; Oct4), AKT1, ALDH1A1 and PROM1 (prominin 1; CD133) and generate a protein interaction network. A total of 15 prominent protein nodes and 65 edges, including MTOR (mechanistic target of rapamycin), FOXO1 (forkhead box O1), RICTOR (RPTOR independent companion of MTOR), NOS3 (nitric oxide synthase 3), HSP90AA1 (heat shock protein 90 kDa alpha, class A member 1), MDM2 (mouse double minute 2), FOXO3 (forkhead box O3), ILK (integrin-linked kinase), PTEN (phosphatase and tensin) and GSK3 β (glycogen synthase kinase 3 beta), were identified in this network (Figure 19). AKT1 was the most interactive protein in this PPI network and connected with 13 protein nodes. We identified AKT1 as a central protein in response to the PME treatment.

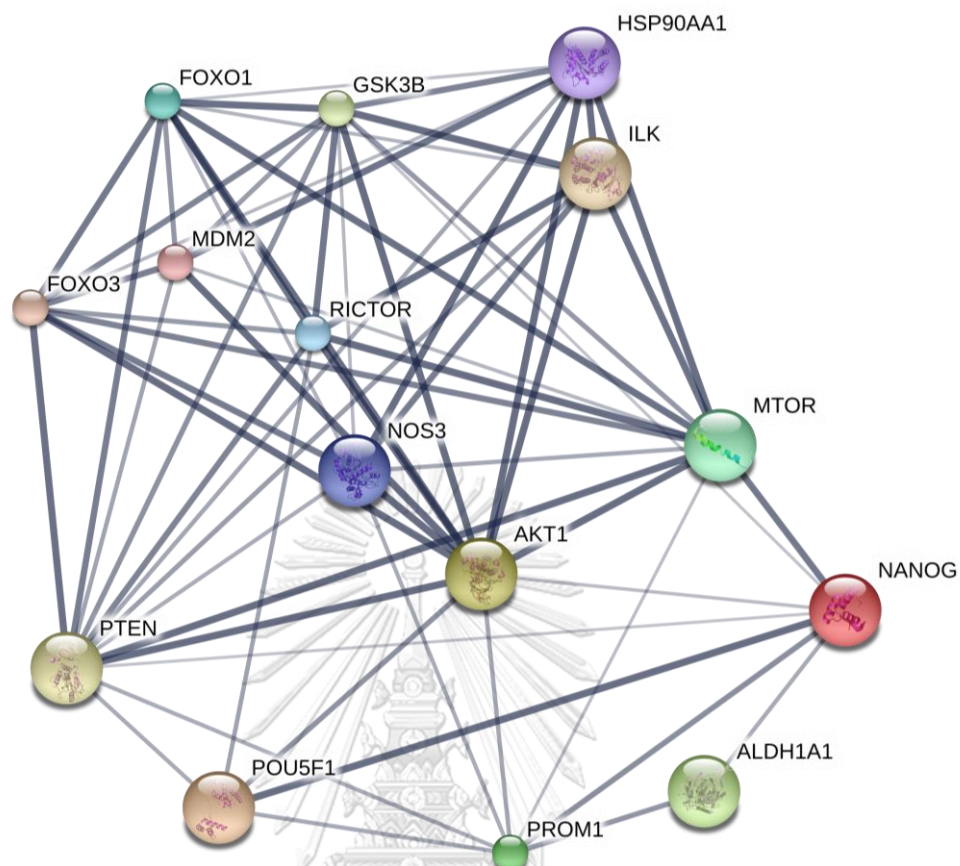


Figure 19 Protein-protein interaction (PPI) networks analysis of the CSC related proteins that affected by PME treatment.

This is the confidence view; network nodes represent proteins, edges represent protein-protein associations, stronger associations are represented by thicker lines, protein-protein interactions are shown in grey, chemical-protein interactions in green and interactions between chemicals in red.

To confirm the protein interaction and underlying pathway of PME treatment. The KEGG mapper (<https://www.genome.jp/kegg/mapper.html>, accessed on 23 July 2021) was utilized to construct the signaling pathway. The KEGG pathways related to the pluripotency of stem cell were identified, namely, 'signaling pathways regulating pluripotency of stem cells' (Figure 20). The KEGG pathway indicated that Akt was an important player in the mechanism of action of PME in the suppression of pluripotent transcription factors (Oct4 and Nanog) *via* the Akt inhibition. Moreover, Figure 20 also suggested other intermediate protein involving in Akt regulating stem cell transcription factors such as T-Box Transcription Factor 3 (Tbx3). In addition, this map suggested the possible upstream regulator of Akt signals including the leukemia inhibitory factor (LIF), fibroblast growth factor 2 (FGF2) and Insulin-like growth factor (IGF). Oct4 and Nanog were represented to be downstream target genes of such pathways that regulate self-renewal and pluripotency maintenance.

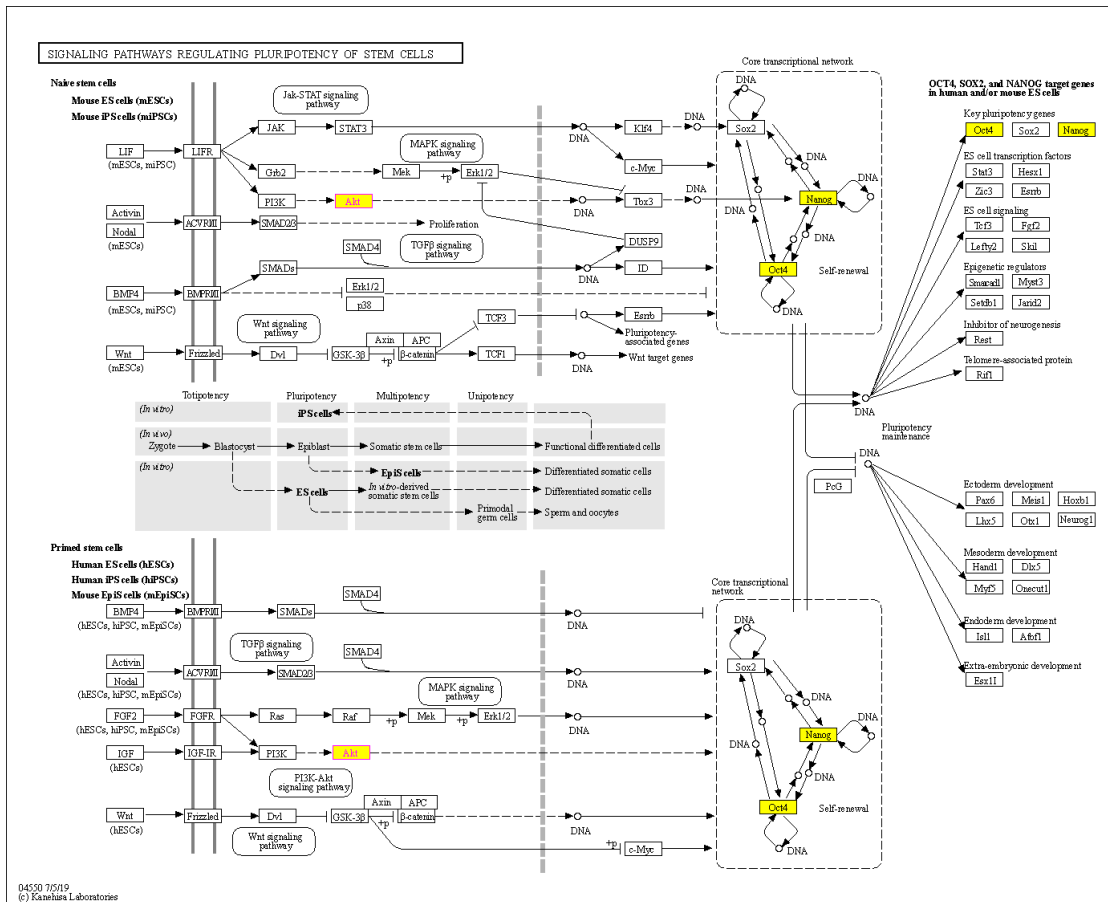


Figure 20 The KEGG pathway

The KEGG mapper database revealed potential Akt up-stream and down-stream signals involved in pluripotency of stem cells. The yellow box represents the proteins affected by PME treatment.

CHAPTER V

DISCUSSION AND CONCLUSION

Lung cancer is the most common cancer worldwide, in which normal epithelial cells undergo genetically damage induced cell proliferation without control in various parts of the lung, and these cancer cells can invade the surrounding tissues and metastasize to the other distant organs (1) (44). CSCs are believed as the underlying cause of the high mortality rate in cancer (17).

In this study, we aimed to understanding the CSCs physiology in clinical of lung cancer patients and determining the CSS-targeting activity of PME to supports the potential use in human lung cancer therapy. First of all, we investigated the CSC behaviors in patient-derived primary NSCLC cells and standard NSCLC cell lines for investigated the CSC phenotypes of all cells. The cell with high ability of CSC would be represented by high CSC phenotypes and highly aggressiveness. The results from Part 1 (Figure 4-7) revealed that H460 cell line as the most aggressive cells and exhibited the highest CSC phenotypes with highly numbers of colony and spheroid formation. The H460 cell line were derived from plural fluid of a patient with large cell cancer of the lung, while the A549 cell line are human alveolar basal epithelial

cells. They are squamous in nature and responsible for the diffusion of substances across the alveoli of lungs (141).

In term of patient-derived primary NSCLC cells group, our study investigates the CSC behaviors in primary lung cancer cells directly derived from advanced stage and recurrent NSCLC patients who had been treated with chemotherapeutic drugs for a prolonged period, which represent to a clinical status in lung cancer patients accurately. The results form part 1 (Figure 4-7) revealed that ELC08 cells had shown great ability of CSCs, which the highest numbers of colony and secondary spheroids formation. ELC10 cells are the second aggressive cells, which the biggest colony and secondary spheroid size. Moreover, ELC10 also presented the highest numbers in primary spheroid formation (Figure 6). ELC17 was the lowest aggressive than the others, which lowest numbers and smallest size of colony and spheroid formation.

The previous study about *in vitro* drug sensitivity testing of malignant pleural effusion from advanced-stage NSCLC patients investigated that, in case ELC08 *in vitro* drug sensitivity testing revealed pan resistance to all potential chemotherapy (gemcitabine, pemetrexed, docetaxel and vinorelbine). The patient's symptoms worsened after 1 cycle of treatment and patient expired 2 weeks after treatment. Case ELC10 *in vitro* drug sensitivity testing revealed resistance to pemetrexed while intermediate response to vinorelbine. Patient had febrile neutropenia and worsening condition prohibited subsequent chemotherapy. Medical pleurodesis was provided

to control patient's symptoms. Case ELC17 the patient's *in vitro* drug sensitivity profile revealed an intermediate response to docetaxel and vinorelbine. In addition, it also showed a resistance pattern to pemetrexed and gemcitabine. Due to poor performance, this patient could not receive subsequent chemotherapy. Intermittent thoracocentesis and the release of pleural effusion was provided (142). Moreover, previous research referred to the limited success on lung cancer treatment, radio-chemotherapy resistant, tumor recurrence and cancer progression that mainly caused by CSCs (8). For the results of drug sensitivity testing study and all patients' characteristics suggested that the resistant primary lung cancer cells represented to high efficiency of CSCs, confirming the reliability of our results of CSC behaviors analysis in part 1 experiment.

CSCs and their related pathways have become potential targets of anti-cancer drugs. Next, we investigated the effect of PME on CSC phenotypes in part 2 experiments. Previous research showed that phenolic compounds, such as vanillin, gigantol and lusianthridin, have the potential to suppress CSCs (143) (42) (144). Gigantol, a bibenzyl compound from *Dendrobium draconis*, suppresses CSC phenotypes in lung cancer cells (42). Vanillin, a major component in *Vanilla planifolia* seed, reduces CSC phenotypes in lung cancer cells and downregulates CSC markers CD133, ALDH1A1 and ABCG2 (143). In addition, lusianthridin, a dihydrophenanthrene compound isolated from the stem of *Dendrobium venustum*,

can suppress lung CSC phenotypes and decrease the levels of CD133, ALDH1A1 and ABCG2 (144).

In this study, we demonstrated for the first time that PME attenuated the CSC phenotypes in human lung cancer cells. The treatment of these cancer cells with PME resulted in their decreased anchorage-independent growth and spheroid formation (Figures 11, 12 and 13). To determine the CSCs, we used CSC markers CD133 and ALDH1A1, which are widely used in the case of lung cancer (13) (57). CSCs were related to the ability of cells to establish survive colonies in an anchorage-independent condition and form detached tumor spheroids (137) (93). We evaluated the expression of such CSC markers in PME-treated cells and observed that PME treatment can reduce CSC markers in concomitant with the suppression of tumor spheroid formation and limited growth in detached condition (Figure 14).

The regulation of CSC properties, such as self-renewal and pluripotency, is modulated by stem-cell transcription factors of normal stem cells and CSCs (19). Oct4 and Nanog are transcription factors that indicate CSC properties in various types of cancers including lung cancer (13) (19). The expressions of Oct4 and Nanog induce spheroid and colony formation (13) (137). Moreover, their expression is related with lung cancer aggressiveness and increases new tumor genesis (60) (61). In this study, Oct4 and Nanog significantly decreased in response to the treatment with PME at non-toxic concentrations (Figure 14).

In terms of upstream signaling pathway, Akt is a cellular signaling pathway that plays a key role in regulating CSC abilities (25). The regulation of CSC transcription factors, including Oct4 and Nanog, showed the downstream regulation of the Akt signaling pathway, causing tumorigenicity and cancer aggressiveness (25) (27). The inhibition of Akt activity attenuated the activity of these transcription factors and other CSC marker proteins, which diminished the resulting CSC phenotypes (25) (29). Previous studies described the potential anti-CSC benefit of CSC transcription factors/Akt pathway inhibition. Srinual et al. reported that vanillin suppresses Oct4 and Nanog expression through the mediation by an Akt-dependent mechanism (143). Gigantol suppresses Oct4 and Nanog reduction through an Akt-dependent mechanism (42). Moreover, both of studies confirm this mechanism using perifosine (1,1-dimethylpiperidinium-4-yl octadecyl phosphate), an Akt inhibitor as a positive control. They treated H460 cells with non-toxic concentrations of perifosine and detect the CSC markers by Western blot analysis. The result revealed that treatment of H460 cells with perifosine significant reduced p-Akt and specific CSCs markers (143) (42). In our findings, PME inhibited CSCs through the reduction of transcription factors Oct4 and Nanog in an Akt-dependent mechanism (Figure 14). To confirm our hypothesis, we performed molecular docking simulations using the ATP-binding site of Akt-1 protein as the target for this compound and investigated Akt-1 interactions compared with the Akt-1 inhibitor (reference compound; CQW). After simulations (Figure 18), the data indicated that the binding affinity of PME was greater than that

of the reference compound and had a similar binding site, which demonstrated the capability of PME to inhibit Akt-1, following previous experimental results.

To further confirm the underlying pathway of PME treatment, we constructed the PPI networks and KEGG pathway maps. To investigate the PPI networks and identify the key protein target of this treatment, using STITCH database, we analyzed the CSC marker proteins that were affected by the PME treatment. We observed that AKT1 was the top protein with the central PPI degree, indicating that PME may exert its CSC-suppressing activity through an Akt-dependent mechanism (Figure 19). In the KEGG pathway map analysis, we recorded that the CSC marker proteins that were affected by the PME treatment were mainly enriched in the signaling pathways regulating the pluripotency of stem cells (Figure 20). This pathway revealed that Akt is an upstream regulator of pluripotent transcription factors Oct4 and Nanog, following the previous experimental results on PME treatment. In addition, this pathway also revealed that LIF, FGF2 and IGF could be upstream regulators of PI3K-Akt signaling pathway. Previous studies indicated that such receptors have an ability to regulate CSCs (145) (146) (147) (148) (149) (150). LIF receptor (LIFR), an upstream regulator of Hippo signaling, has an inversely expressed in relation with miR-125a in human breast cancer stem cells (145). FGF receptor (FGFR), one of the most common growth factors, regulates renewal and differentiation of human embryonic stem cells (hESCs) and CSCs (146) (147). In addition, the IGF signaling was shown to

induce and maintain CSC and epithelial mesenchymal transition (EMT) status (148). Shan et al. reported that Nanog regulates self-renewal of CSCs through the IGF pathway in human hepatocellular carcinoma (149). The inhibition of IGF receptors (IGFR)/Akt/MTOR axis targets colorectal CSCs by attenuating mevalonate-isoprenoid pathway in vitro and in vivo (150). Moreover, this KEGG mapper revealed that Oct4 and Nanog were key pluripotent genes of such pathways to regulate self-renewal and pluripotency maintenance. Most of these proteins that affected by the PME treatment have been reported in lung CSCs, confirming the reliability of the results of bioinformatic analysis.

Furthermore, we confirmed the CSC suppression of this compound in primary lung cells derived from advanced stage and recurrent NSCLC patients who had been treated with chemotherapeutic drugs for a prolonged period, which represent to a clinical status in lung cancer patients accurately and supports the potential use of PME in lung cancer therapy. Previous studies referred to the limited success on lung cancer treatment, radio-chemotherapy resistant, tumor recurrence and cancer progression that mainly caused by CSCs (8). So, it could be said that the resistant primary cancer cells represented to a high efficiency of CSCs. Moreover, study in several cancers indicated that the results of a functional testing in a primary cancer cell could be translated to clinical approaches for measurement of cancer cells response and correlating them to patient responses (151). The results of

immunofluorescence analysis revealed that PME can reduce CSC-specific markers expression (CD133 and Oct4) and suppress spheroid formation in patient-derived NSCLC cells (Figures 13, 16 and 17). Similar with a previous phenolic compound study, it is reported that lusianthridin could suppress CSCs and reduced the ability to form spheroids in primary lung cancer cells (144).

In conclusion, this study reported the novel information of PME in the suppression of CSC phenotypes in human NSCLC cells *via* the inhibition of Akt signaling. The Akt inhibitory effect resulted in the suppression of stem-cell transcription factors and the depletion of CSCs (Figure 21). These data can support the potential use of PME in lung cancer therapy.

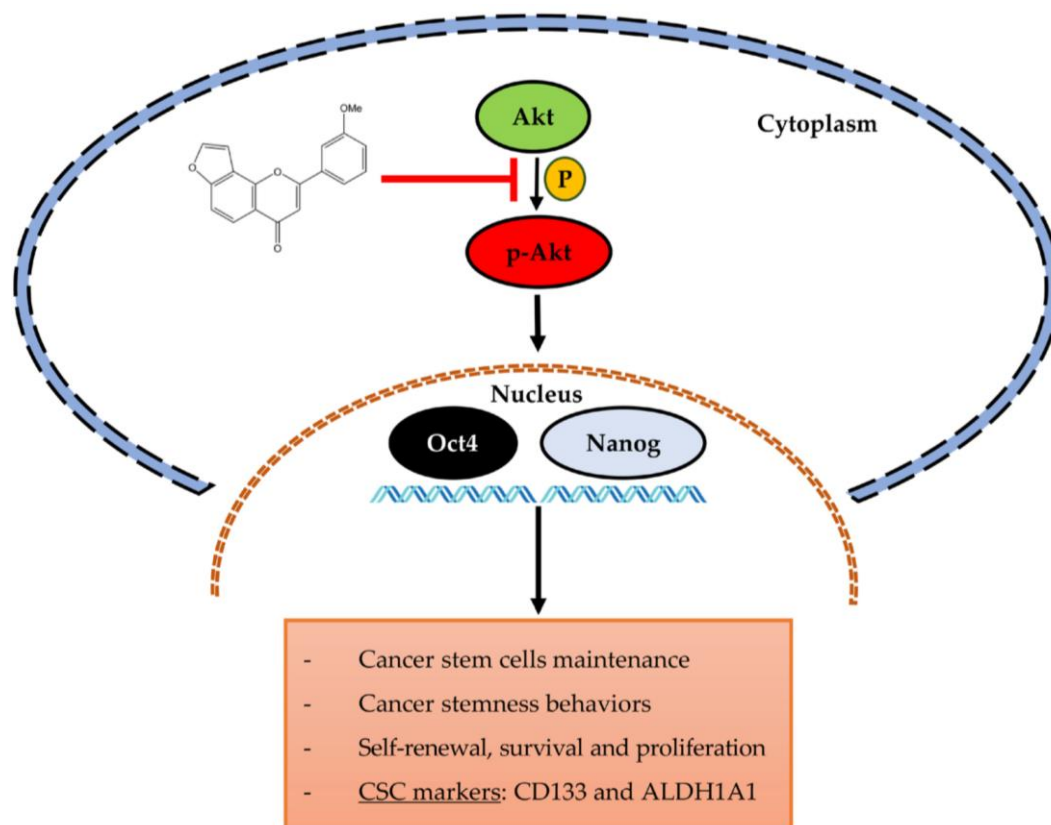


Figure 21 Schematic overview of PME on lung CSC phenotypes and its related pathway.

จุฬาลงกรณ์มหาวิทยาลัย
CHULALONGKORN UNIVERSITY

The schematic representation the attenuation effect of PME on CSC phenotypes and its underlying mechanism pathway in human NSCLC cells.

REFERENCES

1. Bray F, Ferlay J, Soerjomataram I, Siegel RL, Torre LA, Jemal A. Global cancer statistics 2018: GLOBOCAN estimates of incidence and mortality worldwide for 36 cancers in 185 countries. *CA Cancer J Clin.* 2018;68(6):394-424.
2. [int/news-room/fact-sheets/detail/the-top-10-causes-of-death](https://www.who.int/news-room/fact-sheets/detail/the-top-10-causes-of-death) WHOJDNhww. The top 10 causes of death. 24 May 2018. 2019.
3. Torre LA, Siegel RL, Ward EM, Jemal A. Global cancer incidence and mortality rates and trends—an update. *Cancer Epidemiology Prevention Biomarkers.* 2016;25(1):16-27.
4. Moore MA, Yoo KY, Tuncer M, Sobue T. Overview of players and information in the cancer epidemiology and control world in Asia. *Asian Pac J Cancer Prev.* 2010;11 Suppl 2:1-10.
5. Cooper GM, Hausman RE. The development and causes of cancer. *The cell: A molecular approach.* 2000;2.
6. Vogt PK. Cancer genes. *West J Med.* 1993;158(3):273-8.
7. Hanahan D, Weinberg RA. Hallmarks of cancer: the next generation. *Cell.* 2011;144(5):646-74.
8. Chang JC. Cancer stem cells: Role in tumor growth, recurrence, metastasis, and treatment resistance. *Medicine (Baltimore).* 2016;95(1 Suppl 1):S20-S5.
9. Ho MM, Ng AV, Lam S, Hung JY. Side population in human lung cancer cell lines and tumors is enriched with stem-like cancer cells. *Cancer research.* 2007;67(10):4827-33.
10. Pardal R, Clarke MF, Morrison SJ. Applying the principles of stem-cell biology to cancer. *Nat Rev Cancer.* 2003;3(12):895-902.
11. Ayob AZ, Ramasamy TS. Cancer stem cells as key drivers of tumour progression. *Journal of biomedical science.* 2018;25(1):1-18.
12. Kim WT, Ryu CJ. Cancer stem cell surface markers on normal stem cells. *BMB Rep.* 2017;50(6):285-98.
13. Maiuthed A, Chantarawong W, Chanvorachote P. Lung Cancer Stem Cells and

- Cancer Stem Cell-targeting Natural Compounds. *Anticancer Res.* 2018;38(7):3797-809.
14. MacDonagh L, Gray SG, Breen E, Cuffe S, Finn SP, O'Byrne KJ, et al. Lung cancer stem cells: The root of resistance. *Cancer Lett.* 2016;372(2):147-56.
 15. Cortes-Dericks L, Galetta D, Spaggiari L, Schmid RA, Karoubi G. High expression of octamer-binding transcription factor 4A, prominin-1 and aldehyde dehydrogenase strongly indicates involvement in the initiation of lung adenocarcinoma resulting in shorter disease-free intervals. *Eur J Cardiothorac Surg.* 2012;41(6):e173-81.
 16. Nassar D, Blanpain C. Cancer Stem Cells: Basic Concepts and Therapeutic Implications. *Annu Rev Pathol.* 2016;11:47-76.
 17. Toledo-Guzmán ME, Bigoni-Ordóñez GD, Hernández MI, Ortiz-Sánchez E. Cancer stem cell impact on clinical oncology. *World journal of stem cells.* 2018;10(12):183.
 18. Zakaria N, Satar NA, Abu Halim NH, Ngalm SH, Yusoff NM, Lin J, et al. Targeting Lung Cancer Stem Cells: Research and Clinical Impacts. *Front Oncol.* 2017;7:80.
 19. Liu A, Yu X, Liu S. Pluripotency transcription factors and cancer stem cells: small genes make a big difference. *Chinese journal of cancer.* 2013;32(9):483.
 20. Zhu P, Fan Z. Cancer stem cells and tumorigenesis. *Biophys Rep.* 2018;4(4):178-88.
 21. Hambardzumyan D, Becher OJ, Holland EC. Cancer stem cells and survival pathways. *Cell Cycle.* 2008;7(10):1371-8.
 22. Vara JÁF, Casado E, de Castro J, Cejas P, Belda-Iniesta C, González-Barón M. PI3K/Akt signalling pathway and cancer. *Cancer treatment reviews.* 2004;30(2):193-204.
 23. Jiang N, Dai Q, Su X, Fu J, Feng X, Peng J. Role of PI3K/AKT pathway in cancer: the framework of malignant behavior. *Mol Biol Rep.* 2020;47(6):4587-629.
 24. Massion PP, Taflan PM, Shyr Y, Rahman SM, Yildiz P, Shakthour B, et al. Early involvement of the phosphatidylinositol 3-kinase/Akt pathway in lung cancer progression. *Am J Respir Crit Care Med.* 2004;170(10):1088-94.
 25. Rivas S, Gomez-Oro C, Anton IM, Wandosell F. Role of Akt Isoforms Controlling Cancer Stem Cell Survival, Phenotype and Self-Renewal. *Biomedicines.* 2018;6(1):29.
 26. Kim JS, Kim BS, Kim J, Park CS, Chung IY. The phosphoinositide-3-kinase/Akt pathway mediates the transient increase in Nanog expression during differentiation of F9 cells. *Arch Pharm Res.* 2010;33(7):1117-25.

27. Yoon C, Lu J, Yi BC, Chang KK, Simon MC, Ryeom S, et al. PI3K/Akt pathway and Nanog maintain cancer stem cells in sarcomas. *Oncogenesis*. 2021;10(1):12.
28. Zhao QW, Zhou YW, Li WX, Kang B, Zhang XQ, Yang Y, et al. Akt-mediated phosphorylation of Oct4 is associated with the proliferation of stem-like cancer cells. *Oncology Reports*. 2015;33(4):1621-9.
29. Li W, Zhou Y, Zhang X, Yang Y, Dan S, Su T, et al. Dual inhibiting OCT4 and AKT potently suppresses the propagation of human cancer cells. *Sci Rep*. 2017;7(1):46246.
30. Lemjabbar-Alaoui H, Hassan OU, Yang YW, Buchanan P. Lung cancer: Biology and treatment options. *Biochim Biophys Acta*. 2015;1856(2):189-210.
31. Hammerschmidt S, Wirtz H. Lung cancer: current diagnosis and treatment. *Dtsch Arztebl Int*. 2009;106(49):809-18; quiz 19-20.
32. Miller KD, Nogueira L, Mariotto AB, Rowland JH, Yabroff KR, Alfano CM, et al. Cancer treatment and survivorship statistics, 2019. *CA Cancer J Clin*. 2019;69(5):363-85.
33. Di C, Zhao Y. Multiple drug resistance due to resistance to stem cells and stem cell treatment progress in cancer. *Experimental therapeutic medicine*. 2015;9(2):289-93.
34. Sritularak B, Likhitwitayawuid K, Conrad J, Vogler B, Reeb S, Klaiber I, et al. New Flavones from *Millettia erythrocalyx*. *Journal of Natural Products*. 2002;65(4):589-91.
35. Jena R, Rath D, Rout SS, Kar DM. A review on genus *Millettia*: Traditional uses, phytochemicals and pharmacological activities. *Saudi Pharmaceutical Journal*. 2020;28(12):1686.
36. Likhitwitayawuid K, Sritularak B, Benchanak K, Lipipun V, Mathew J, Schinazi RF. Phenolics with antiviral activity from *Millettia erythrocalyx* and *Artocarpus lakoocha*. *Nat Prod Res*. 2005;19(2):177-82.
37. Fonseca BF, Predes D, Cerqueira DM, Reis AH, Amado NG, Cayres MC, et al. Derricin and derricidin inhibit Wnt/ β -catenin signaling and suppress colon cancer cell growth in vitro. *PLoS One*. 2015;10(3):e0120919.
38. Mansoor TA, Ramalho RM, Luo X, Ramalhete C, Rodrigues CM, Ferreira MJU. Isoflavones as apoptosis inducers in human hepatoma HuH-7 cells. *Phytotherapy Research*. 2011;25(12):1819-24.
39. Vetrivel P, Kim SM, Ha SE, Kim HH, Bhosale PB, Senthil K, et al. Compound

Prunetin Induces Cell Death in Gastric Cancer Cell with Potent Anti-Proliferative Properties: In Vitro Assay, Molecular Docking, Dynamics, and ADMET Studies. *Biomolecules*. 2020;10(7):1086.

40. Balijepalli MK, Tandra S, Pichika MR. Antiproliferative activity and induction of apoptosis in estrogen receptor-positive and negative human breast carcinoma cell lines by *Gmelina asiatica* roots. *Pharmacognosy research*. 2010;2(2):113.

41. Cai C, Zhu X. The Wnt/ β -catenin pathway regulates self-renewal of cancer stem-like cells in human gastric cancer. *Molecular medicine reports*. 2012;5(5):1191-6.

42. Bhummaphan N, Chanvorachote P. Gigantol Suppresses Cancer Stem Cell-Like Phenotypes in Lung Cancer Cells. *Evid Based Complement Alternat Med*. 2015;2015:836564.

43. Bhummaphan N, Pongrakhananon V, Sritularak B, Chanvorachote P. Cancer stem cell-suppressing activity of chrysotoxine, a bibenzyl from *Dendrobium pulchellum*. *Journal of Pharmacology Experimental Therapeutics*. 2018;364(2):332-46.

44. Sutherland KD, Berns A. Cell of origin of lung cancer. *Mol Oncol*. 2010;4(5):397-403.

45. Malhotra J, Malvezzi M, Negri E, La Vecchia C, Boffetta P. Risk factors for lung cancer worldwide. *Eur Respir J*. 2016;48(3):889-902.

46. Siddiqui MA, Gollavilli PN, Ramesh V, Parma B, Schwab A, Vazakidou ME, et al. Thymidylate synthase drives the phenotypes of epithelial-to-mesenchymal transition in non-small cell lung cancer. *Br J Cancer*. 2021;124(1):281-9.

47. Basumallik N, Agarwal M. Cancer, lung small cell (oat cell). *StatPearls*. 2019.

48. van Meerbeeck JP, Fennell DA, De Ruyscher DK. Small-cell lung cancer. *Lancet*. 2011;378(9804):1741-55.

49. Ettinger DS, Akerley W, Bepler G, Blum MG, Chang A, Cheney RT, et al. Non-small cell lung cancer. *Journal of the national comprehensive cancer network*. 2010;8(7):740-801.

50. Clark SB, Alsubait S. Non Small Cell Lung Cancer. *StatPearls*. 2020.

51. Mullangi S, Lekkala MR. Adenocarcinoma. *StatPearls*. 2020.

52. Myers DJ, Wallen JM. Cancer, lung adenocarcinoma. *StatPearls*. 2020.

53. Sabbula BR, Anjum F. Squamous Cell Lung Cancer. StatPearls. 2020.
54. Rajdev K, Siddiqui AH, Ibrahim U, Patibandla P, Khan T, El-Sayegh D. An Unusually Aggressive Large Cell Carcinoma of the Lung: Undiagnosed until Autopsy. Cureus. 2018;10(2):e2202.
55. Phi LTH, Sari IN, Yang Y-G, Lee S-H, Jun N, Kim KS, et al. Cancer stem cells (CSCs) in drug resistance and their therapeutic implications in cancer treatment. Stem cells international. 2018;2018.
56. Leon G, MacDonagh L, Finn SP, Cuffe S, Barr MP. Cancer stem cells in drug resistant lung cancer: Targeting cell surface markers and signaling pathways. Pharmacol Ther. 2016;158:71-90.
57. Roudi R, Korourian A, Sharifabrizi A, Madjd Z. Differential expression of cancer stem cell markers ALDH1 and CD133 in various lung cancer subtypes. Cancer investigation. 2015;33(7):294-302.
58. Mehta P, Novak C, Raghavan S, Ward M, Mehta G. Self-renewal and CSCs in vitro enrichment: growth as floating spheres. Cancer Stem Cells: Springer; 2018. p. 61-75.
59. Heryanto YD, Achmad A, Taketomi-Takahashi A, Tsushima Y. In vivo molecular imaging of cancer stem cells. Am J Nucl Med Mol Imaging. 2015;5(1):14-26.
60. Zhao C, Setrerrahmane S, Xu H. Enrichment and characterization of cancer stem cells from a human non-small cell lung cancer cell line. Oncol Rep. 2015;34(4):2126-32.
61. Wang P, Gao Q, Suo Z, Munthe E, Solberg S, Ma L, et al. Identification and characterization of cells with cancer stem cell properties in human primary lung cancer cell lines. PLoS One. 2013;8(3):e57020.
62. Salnikov AV, Gladkich J, Moldenhauer G, Volm M, Mattern J, Herr I. CD133 is indicative for a resistance phenotype but does not represent a prognostic marker for survival of non-small cell lung cancer patients. International journal of cancer. 2010;126(4):950-8.
63. Jiang F, Qiu Q, Khanna A, Todd NW, Deepak J, Xing L, et al. Aldehyde dehydrogenase 1 is a tumor stem cell-associated marker in lung cancer. Molecular cancer research. 2009;7(3):330-8.
64. Chiou S-H, Wang M-L, Chou Y-T, Chen C-J, Hong C-F, Hsieh W-J, et al.

Coexpression of Oct4 and Nanog enhances malignancy in lung adenocarcinoma by inducing cancer stem cell-like properties and epithelial-mesenchymal transdifferentiation. *Cancer research*. 2010;70(24):10433-44.

65. Du Y, Ma C, Wang Z, Liu Z, Liu H, Wang T. Nanog, a novel prognostic marker for lung cancer. *Surg Oncol*. 2013;22(4):224-9.

66. Karoubi G, Gugger M, Schmid R, Dutly A. OCT4 expression in human non-small cell lung cancer: implications for therapeutic intervention. *Interact Cardiovasc Thorac Surg*. 2009;8(4):393-7.

67. Jeter CR, Yang T, Wang J, Chao HP, Tang DG. Concise Review: NANOG in Cancer Stem Cells and Tumor Development: An Update and Outstanding Questions. *Stem Cells*. 2015;33(8):2381-90.

68. Iv Santaliz-Ruiz LE, Xie X, Old M, Teknos TN, Pan Q. Emerging role of nanog in tumorigenesis and cancer stem cells. *Int J Cancer*. 2014;135(12):2741-8.

69. Linn DE, Yang X, Sun F, Xie Y, Chen H, Jiang R, et al. A Role for OCT4 in Tumor Initiation of Drug-Resistant Prostate Cancer Cells. *Genes Cancer*. 2010;1(9):908-16.

70. Hayashi H, Arai T, Togashi Y, Kato H, Fujita Y, De Velasco M, et al. The OCT4 pseudogene POU5F1B is amplified and promotes an aggressive phenotype in gastric cancer. *Oncogene*. 2015;34(2):199-208.

71. Glumac PM, LeBeau AM. The role of CD133 in cancer: a concise review. *Clin Transl Med*. 2018;7(1):18.

72. Codony-Servat J, Verlicchi A, Rosell R. Cancer stem cells in small cell lung cancer. *Transl Lung Cancer Res*. 2016;5(1):16-25.

73. Le H, Zeng F, Xu L, Liu X, Huang Y. The role of CD133 expression in the carcinogenesis and prognosis of patients with lung cancer. *Mol Med Rep*. 2013;8(5):1511-8.

74. Huang M, Zhu H, Feng J, Ni S, Huang J. High CD133 expression in the nucleus and cytoplasm predicts poor prognosis in non-small cell lung cancer. *Dis Markers*. 2015;2015:986095.

75. Ahmed Laskar A, Younus H. Aldehyde toxicity and metabolism: the role of aldehyde dehydrogenases in detoxification, drug resistance and carcinogenesis. *Drug Metab Rev*. 2019;51(1):42-64.

76. Lindahl R. Aldehyde dehydrogenases and their role in carcinogenesis. *Critical reviews in biochemistry molecular biology*. 1992;27(4-5):283-335.
77. Muzio G, Maggiora M, Paiuzzi E, Oraldi M, Canuto RA. Aldehyde dehydrogenases and cell proliferation. *Free Radic Biol Med*. 2012;52(4):735-46.
78. Li X, Wan L, Geng J, Wu CL, Bai X. Aldehyde dehydrogenase 1A1 possesses stem-like properties and predicts lung cancer patient outcome. *J Thorac Oncol*. 2012;7(8):1235-45.
79. Clark DW, Palle K. Aldehyde dehydrogenases in cancer stem cells: potential as therapeutic targets. *Annals of translational medicine*. 2016;4(24).
80. Huang CP, Tsai MF, Chang TH, Tang WC, Chen SY, Lai HH, et al. ALDH-positive lung cancer stem cells confer resistance to epidermal growth factor receptor tyrosine kinase inhibitors. *Cancer Lett*. 2013;328(1):144-51.
81. Liu J, Xiao Z, Wong SK-M, Tin VP-C, Ho K-Y, Wang J, et al. Lung cancer tumorigenicity and drug resistance are maintained through ALDHhiCD44hi tumor initiating cells. *Oncotarget*. 2013;4(10):1698.
82. Wang ML, Chiou SH, Wu CW. Targeting cancer stem cells: emerging role of Nanog transcription factor. *Onco Targets Ther*. 2013;6:1207-20.
83. Suresh R, Ali S, Ahmad A, Philip PA, Sarkar FHJLc, therapies pmn, et al. The role of cancer stem cells in recurrent and drug-resistant lung cancer. 2016:57-74.
84. Gawlik-Rzemieniewska N, Bednarek I. The role of NANOG transcriptional factor in the development of malignant phenotype of cancer cells. *Cancer Biol Ther*. 2016;17(1):1-10.
85. Cheng W, Wang H, Yuan J, Cheng Z, Xing D, Zhang M. The Prognostic Value of Nanog Overexpression in Lung Cancer: A Meta-Analysis. *Biomed Res Int*. 2018;2018:3429261.
86. Zhang Q, Han Z, Zhu Y, Chen J, Li W. The Role and Specific Mechanism of OCT4 in Cancer Stem Cells: A Review. *Int J Stem Cells*. 2020;13(3):312-25.
87. Kumar SM, Liu S, Lu H, Zhang H, Zhang PJ, Gimotty PA, et al. Acquired cancer stem cell phenotypes through Oct4-mediated dedifferentiation. *Oncogene*. 2012;31(47):4898-911.
88. Wang YJ, Herlyn M. The emerging roles of Oct4 in tumor-initiating cells. *Am J*

Physiol Cell Physiol. 2015;309(11):C709-18.

89. Li H, Wang L, Shi S, Xu Y, Dai X, Li H, et al. The Prognostic and Clinicopathologic Characteristics of OCT4 and Lung Cancer: A Meta-Analysis. *Curr Mol Med*. 2019;19(1):54-75.
90. Li SJ, Huang J, Zhou XD, Zhang WB, Lai YT, Che GW. Clinicopathological and prognostic significance of Oct-4 expression in patients with non-small cell lung cancer: a systematic review and meta-analysis. *J Thorac Dis*. 2016;8(7):1587-600.
91. Zhang X, Han B, Huang J, Zheng B, Geng Q, Aziz F, et al. Prognostic significance of OCT4 expression in adenocarcinoma of the lung. *Jpn J Clin Oncol*. 2010;40(10):961-6.
92. Mohiuddin IS, Wei SJ, Kang MH. Role of OCT4 in cancer stem-like cells and chemotherapy resistance. *Biochim Biophys Acta Mol Basis Dis*. 2020;1866(4):165432.
93. Chanvorachote P, Luanpitpong S. Iron induces cancer stem cells and aggressive phenotypes in human lung cancer cells. *Am J Physiol Cell Physiol*. 2016;310(9):C728-39.
94. Zhang XY, Dong QG, Huang JS, Huang AM, Shi CL, Jin B, et al. The expression of stem cell-related indicators as a prognostic factor in human lung adenocarcinoma. *Journal of surgical oncology*. 2010;102(7):856-62.
95. Qu H, Li R, Liu Z, Zhang J, Luo R. Prognostic value of cancer stem cell marker CD133 expression in non-small cell lung cancer: a systematic review. *Int J Clin Exp Pathol*. 2013;6(11):2644-50.
96. Ma I, Allan AL. The role of human aldehyde dehydrogenase in normal and cancer stem cells. *Stem Cell Rev Rep*. 2011;7(2):292-306.
97. Ponta H, Sherman L, Herrlich PA. CD44: from adhesion molecules to signalling regulators. *Nat Rev Mol Cell Biol*. 2003;4(1):33-45.
98. Leung EL, Fiscus RR, Tung JW, Tin VP, Cheng LC, Sihoe AD, et al. Non-small cell lung cancer cells expressing CD44 are enriched for stem cell-like properties. *PLoS One*. 2010;5(11):e14062.
99. Ding XW, Wu JH, Jiang CP. ABCG2: a potential marker of stem cells and novel target in stem cell and cancer therapy. *Life Sci*. 2010;86(17-18):631-7.
100. Liang SC, Yang CY, Tseng JY, Wang HL, Tung CY, Liu HW, et al. ABCG2 localizes to the nucleus and modulates CDH1 expression in lung cancer cells. *Neoplasia*.

2015;17(3):265-78.

101. Wefers C, Schreibelt G, Massuger L, de Vries IJM, Torensma R. Immune Curbing of Cancer Stem Cells by CTLs Directed to NANOG. *Front Immunol.* 2018;9:1412.
102. Sarkar A, Hochedlinger KJ. The sox family of transcription factors: versatile regulators of stem and progenitor cell fate. 2013;12(1):15-30.
103. Weina K, Utikal J. SOX2 and cancer: current research and its implications in the clinic. *Clin Transl Med.* 2014; 3: 19. Epub 2014/08/13. doi: 10.1186/2001-1326-3-19 PMID: 25114775.
104. Lien EC, Dibble CC, Toker A. PI3K signaling in cancer: beyond AKT. *Curr Opin Cell Biol.* 2017;45:62-71.
105. Vivanco I, Sawyers CL. The phosphatidylinositol 3-kinase–AKT pathway in human cancer. *Nature Reviews Cancer.* 2002;2(7):489-501.
106. Frost RA, Lang CH. Protein kinase B/Akt: a nexus of growth factor and cytokine signaling in determining muscle mass. *J Appl Physiol (1985).* 2007;103(1):378-87.
107. Yang ZZ, Tschopp O, Baudry A, Dummler B, Hynx D, Hemmings BA. Physiological functions of protein kinase B/Akt. *Biochem Soc Trans.* 2004;32(Pt 2):350-4.
108. Vasudevan KM, Garraway LA. AKT signaling in physiology and disease. *Curr Top Microbiol Immunol.* 2010;347:105-33.
109. Fumarola C, Bonelli MA, Petronini PG, Alfieri RR. Targeting PI3K/AKT/mTOR pathway in non small cell lung cancer. *Biochem Pharmacol.* 2014;90(3):197-207.
110. Brognard J, Clark AS, Ni Y, Dennis PA. Akt/protein kinase B is constitutively active in non-small cell lung cancer cells and promotes cellular survival and resistance to chemotherapy and radiation. *Cancer research.* 2001;61(10):3986-97.
111. Kandel ES, Hay N. The regulation and activities of the multifunctional serine/threonine kinase Akt/PKB. *Exp Cell Res.* 1999;253(1):210-29.
112. Kohn AD, Barthel A, Kovacina KS, Boge A, Wallach B, Summers SA, et al. Construction and characterization of a conditionally active version of the serine/threonine kinase Akt. *J Biol Chem.* 1998;273(19):11937-43.
113. Porter AC, Vaillancourt RR. Tyrosine kinase receptor-activated signal transduction pathways which lead to oncogenesis. *Oncogene.* 1998;17(11):1343-52.
114. Xia P, Xu XY. PI3K/Akt/mTOR signaling pathway in cancer stem cells: from basic

research to clinical application. *Am J Cancer Res.* 2015;5(5):1602-9.

115. Reya T, Morrison SJ, Clarke MF, Weissman IL. Stem cells, cancer, and cancer stem cells. *Nature.* 2001;414(6859):105-11.
116. Hassan G, Du J, Afify SM, Seno A, Seno M. Cancer stem cell generation by silenced MAPK enhancing PI3K/AKT signaling. *Med Hypotheses.* 2020;141:109742.
117. Martelli AM, Tazzari PL, Evangelisti C, Chiarini F, Blalock WL, Billi AM, et al. Targeting the phosphatidylinositol 3-kinase/Akt/mammalian target of rapamycin module for acute myelogenous leukemia therapy: from bench to bedside. *Curr Med Chem.* 2007;14(19):2009-23.
118. Altomare DA, Testa JR. Perturbations of the AKT signaling pathway in human cancer. *Oncogene.* 2005;24(50):7455-64.
119. Testa JR, Bellacosa A. AKT plays a central role in tumorigenesis. *Proc Natl Acad Sci U S A.* 2001;98(20):10983-5.
120. Sharma SV, Haber DA, Settleman J. Cell line-based platforms to evaluate the therapeutic efficacy of candidate anticancer agents. *Nat Rev Cancer.* 2010;10(4):241-53.
121. Ben-David U, Beroukhim R, Golub TR. Genomic evolution of cancer models: perils and opportunities. *Nat Rev Cancer.* 2019;19(2):97-109.
122. Gazdar AF, Gao B, Minna JD. Lung cancer cell lines: Useless artifacts or invaluable tools for medical science? *Lung Cancer.* 2010;68(3):309-18.
123. Kirk R. Genetics: Personalized medicine and tumour heterogeneity. *Nat Rev Clin Oncol.* 2012;9(5):250.
124. Wistuba II, Bryant D, Behrens C, Milchgrub S, Virmani AK, Ashfaq R, et al. Comparison of features of human lung cancer cell lines and their corresponding tumors. *Clinical cancer research.* 1999;5(5):991-1000.
125. Jiang Y, Zhao J, Zhang Y, Li K, Li T, Chen X, et al. Establishment of lung cancer patient-derived xenograft models and primary cell lines for lung cancer study. *J Transl Med.* 2018;16(1):138.
126. Burley SK, Bhikadiya C, Bi C, Bittrich S, Chen L, Crichlow GV, et al. RCSB Protein Data Bank: powerful new tools for exploring 3D structures of biological macromolecules for basic and applied research and education in fundamental biology, biomedicine, biotechnology, bioengineering and energy sciences. *Nucleic Acids Res.*

2021;49(D1):D437-D51.

127. Lippa B, Pan G, Corbett M, Li C, Kauffman GS, Pandit J, et al. Synthesis and structure based optimization of novel Akt inhibitors. *Bioorg Med Chem Lett*. 2008;18(11):3359-63.

128. Pettersen EF, Goddard TD, Huang CC, Meng EC, Couch GS, Croll TI, et al. UCSF ChimeraX: Structure visualization for researchers, educators, and developers. *Protein Sci*. 2021;30(1):70-82.

129. Word JM, Lovell SC, Richardson JS, Richardson DC. Asparagine and glutamine: using hydrogen atom contacts in the choice of side-chain amide orientation. *J Mol Biol*. 1999;285(4):1735-47.

130. Ravindranath PA, Forli S, Goodsell DS, Olson AJ, Sanner MF. AutoDockFR: Advances in Protein-Ligand Docking with Explicitly Specified Binding Site Flexibility. *PLoS Comput Biol*. 2015;11(12):e1004586.

131. Kim S, Chen J, Cheng T, Gindulyte A, He J, He S, et al. PubChem in 2021: new data content and improved web interfaces. *Nucleic Acids Res*. 2021;49(D1):D1388-D95.

132. Frisch MJ. Gaussian09. <http://www.gaussian.com/>.

133. Trott O, Olson AJ. AutoDock Vina: improving the speed and accuracy of docking with a new scoring function, efficient optimization, and multithreading. *J Comput Chem*. 2010;31(2):455-61.

134. Nguyen NT, Nguyen TH, Pham TNH, Huy NT, Bay MV, Pham MQ, et al. Autodock vina adopts more accurate binding poses but autodock4 forms better binding affinity. *J Chem Inf Model*. 2019;60(1):204-11.

135. Forli S, Huey R, Pique ME, Sanner MF, Goodsell DS, Olson AJ. Computational protein–ligand docking and virtual drug screening with the AutoDock suite. *Nat Protoc*. 2016;11(5):905-19.

136. Gao W, Wu D, Wang Y, Wang Z, Zou C, Dai Y, et al. Development of a novel and economical agar-based non-adherent three-dimensional culture method for enrichment of cancer stem-like cells. *Stem Cell Res Ther*. 2018;9(1):243.

137. Braunholz D, Saki M, Niehr F, Ozturk M, Borrás Puertolas B, Konschak R, et al. Spheroid Culture of Head and Neck Cancer Cells Reveals an Important Role of EGFR Signalling in Anchorage Independent Survival. *PLoS One*. 2016;11(9):e0163149.

138. Boo L, Ho WY, Ali NM, Yeap SK, Ky H, Chan KG, et al. MiRNA Transcriptome Profiling of Spheroid-Enriched Cells with Cancer Stem Cell Properties in Human Breast MCF-7 Cell Line. *Int J Biol Sci.* 2016;12(4):427-45.
139. Kaseb HO, Fohrer-Ting H, Lewis DW, Lagasse E, Gollin SM. Identification, expansion and characterization of cancer cells with stem cell properties from head and neck squamous cell carcinomas. *Exp Cell Res.* 2016;348(1):75-86.
140. Cleves AE, Jain AN. Knowledge-guided docking: accurate prospective prediction of bound configurations of novel ligands using Surflex-Dock. *J Comput Aided Mol Des.* 2015;29(6):485-509.
141. Gazdar AF, Girard L, Lockwood WW, Lam WL, Minna JD. Lung cancer cell lines as tools for biomedical discovery and research. *Journal of the National Cancer Institute.* 2010;102(17):1310-21.
142. Vinayanuwattikun C, Prakhongcheep O, Tungsukruthai S, Petsri K, Thirasastr P, Leelayuwatanakul N, et al. Feasibility Technique of Low-passage In Vitro Drug Sensitivity Testing of Malignant Pleural Effusion from Advanced-stage Non-small Cell Lung Cancer for Prediction of Clinical Outcome. *Anticancer Res.* 2019;39(12):6981-8.
143. Srinual S, Chanvorachote P, Pongrakhananon V. Suppression of cancer stem-like phenotypes in NCI-H460 lung cancer cells by vanillin through an Akt-dependent pathway. *International journal of oncology.* 2017;50(4):1341-51.
144. Bhummaphan N, Petpiroon N, Prakhongcheep O, Sritularak B, Chanvorachote P. Lusianthridin targeting of lung cancer stem cells via Src-STAT3 suppression. *Phytomedicine.* 2019;62:152932.
145. Nandy SB, Arumugam A, Subramani R, Pedroza D, Hernandez K, Saltzstein E, et al. MicroRNA-125a influences breast cancer stem cells by targeting leukemia inhibitory factor receptor which regulates the Hippo signaling pathway. *Oncotarget.* 2015;6(19):17366.
146. Dvorak P, Dvorakova D, Hampl A. Fibroblast growth factor signaling in embryonic and cancer stem cells. *FEBS Lett.* 2006;580(12):2869-74.
147. Meng Y, Bai X, Huang Y, He L, Zhang Z, Li X, et al. Basic fibroblast growth factor signalling regulates cancer stem cells in lung cancer A549 cells. *J Pharm Pharmacol.* 2019;71(9):1412-20.

148. Malaguarnera R, Belfiore A. The emerging role of insulin and insulin-like growth factor signaling in cancer stem cells. *Front Endocrinol (Lausanne)*. 2014;5:10.
149. Shan J, Shen J, Liu L, Xia F, Xu C, Duan G, et al. Nanog regulates self-renewal of cancer stem cells through the insulin-like growth factor pathway in human hepatocellular carcinoma. *Hepatology*. 2012;56(3):1004-14.
150. Sharon C, Baranwal S, Patel NJ, Rodriguez-Agudo D, Pandak WM, Majumdar AP, et al. Inhibition of insulin-like growth factor receptor/AKT/mammalian target of rapamycin axis targets colorectal cancer stem cells by attenuating mevalonate-isoprenoid pathway in vitro and in vivo. *Oncotarget*. 2015;6(17):15332-47.
151. Pemovska T, Kontro M, Yadav B, Edgren H, Eldfors S, Sz wajda A, et al. Individualized systems medicine strategy to tailor treatments for patients with chemorefractory acute myeloid leukemia. *Cancer discovery*. 2013;3(12):1416-29.





จุฬาลงกรณ์มหาวิทยาลัย
CHULALONGKORN UNIVERSITY

VITA

NAME Sub.Lt.Arnon Silapech

DATE OF BIRTH 18 march 1990

PLACE OF BIRTH Nan, Thailand

INSTITUTIONS ATTENDED Bachelor of Science Program in Emergency Medical Operation, Faculty of Medicine, Mahasarakham University, Thailand

HOME ADDRESS Naval Operational Medicine School, Naval Medical Department, Royal Thai Navy

PUBLICATION Silapech A, Racha S, Aksorn N, Lafauy P, Tungsukruthai S, Vinayanuwattikun C, Sritularak B, Chanvorachote P. Pongol Methyl Ether Inhibits Akt and Suppresses Cancer Stem Cell Phenotypes in Lung Cancer Cells. *Pharmaceuticals*. 2021; 14(11):1085. <https://doi.org/10.3390/ph14111085>